CryoSat-2 satellite radar altimetry for river analysis and modelling

Schneider, Raphael; Bauer-Gottwein, Peter; Madsen, Henrik

Publication date:
2017

Document Version
Publisher's PDF, also known as Version of record

CryoSat-2 satellite radar altimetry for river analysis and modelling

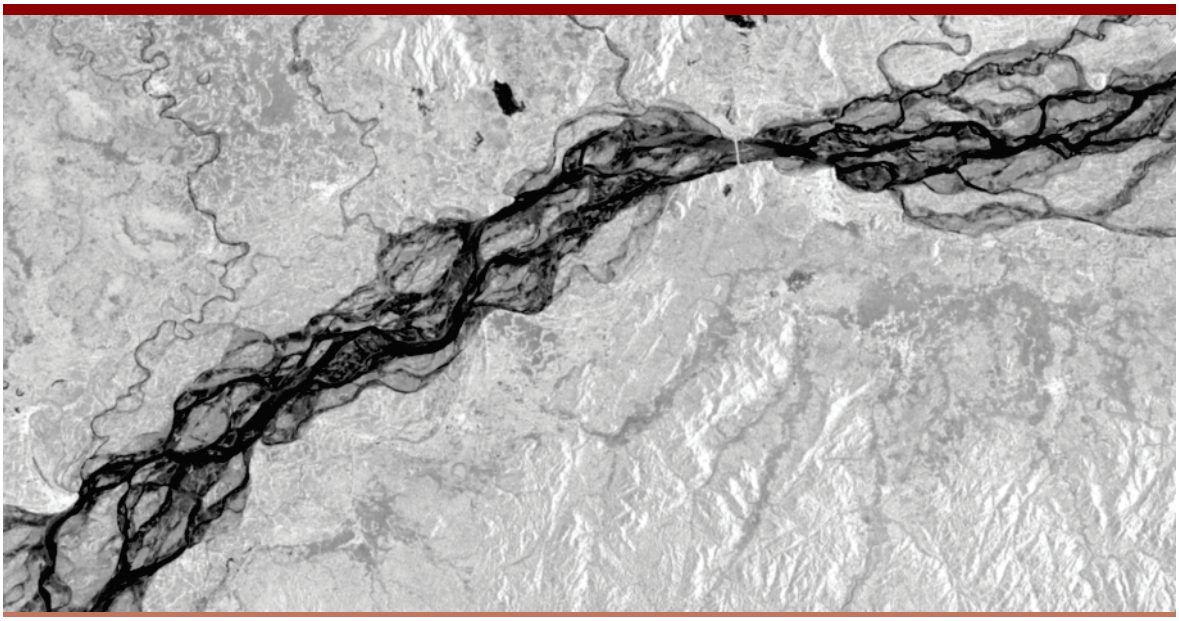

Raphael Schneider

PhD Thesis
September 2017

DTU Environment
Department of Environmental Engineering

CryoSat-2 satellite radar altimetry for river analysis and modelling

Raphael Schneider

PhD Thesis
September 2017

DTU Environment
Department of Environmental Engineering
Technical University of Denmark

CryoSat-2 satellite radar altimetry for river analysis and modelling

Raphael Schneider

PhD Thesis, September 2017

Address: DTU Environment
Department of Environmental Engineering
Technical University of Denmark
Miljoevej, building 113
2800 Kgs. Lyngby
Denmark

Phone reception: +45 4525 1600
Fax: +45 4593 2850

Homepage: http://www.env.dtu.dk
E-mail: reception@env.dtu.dk

Cover photo: Sentinel-1A SAR imagery over the Brahmaputra River
Cover: GraphicCo

Preface

The work presented in this PhD thesis was carried out at the Department of Environmental Engineering at the Technical University of Denmark (DTU) from April 2014 to August 2017. Professor Peter Bauer-Gottwein acted as main supervisor, and Adjunct Professor Henrik Madsen (DHI) as co-supervisor. The work was partly funded by the LOTUS – Preparing Sentinel-3 SAR Altimetry Processing for Ocean and Land project (EU FP7, grant no. 313238) and the CryoSat-2 Success over Inland Water and Land (CRUCIAL) project (ITT ESRIN/AO/1-6827/11/I-NB).

During the PhD study, four scientific journal papers have been prepared, of which two are published. These are listed below and will be referred to in the thesis text by their paper number (e.g. Paper I).

I Jiang, L., Schneider, R., Andersen, O.B., Bauer-Gottwein, P., 2017. CryoSat-2 Altimetry Applications over Rivers and Lakes. Water 9, 211. doi:10.3390/w9030211

II Schneider, R., Tarpanelli, A., Nielsen, K., Madsen, H., Bauer-Gottwein, P. Evaluation of multi-mode CryoSat-2 altimetry data over the Po River against in situ data and a hydrodynamic model. *Manuscript submitted to Adv. Water Resour.*

III Schneider, R., Godiksen, P.N., Villadsen, H., Madsen, H., Bauer-Gottwein, P., 2017. Application of CryoSat-2 altimetry data for river analysis and modelling. Hydrol. Earth Syst. Sci. 21, 751–764. doi:10.5194/hess-21-751-2017

IV Schneider, R., Ridler, M.-E., Godiksen, P.N., Madsen, H., Bauer-Gottwein, P. A data assimilation system combining CryoSat-2 data and hydrodynamic river models. *Under revision. J. Hydrol.*

In this online version of the thesis, papers **I-IV** are not included but can be obtained from electronic article databases e.g. via www.orbit.dtu.dk or on request from DTU Environment, Technical University of Denmark, Miljoevej, Building 113, 2800 Kgs. Lyngby, Denmark, info@env.dtu.dk.

In addition, the following publication, not included in this thesis, was also concluded during this PhD study:

Schneider, R., Godiksen, P.N., Ridler, M.-E., Villadsen, H., Madsen, H., Bauer-Gottwein, P., 2016. Combining Envisat type and CryoSat-2 altimetry to inform hydrodynamic models, in: Ouwehand, L. (Ed.), Proceedings Living Planet Symposium 2016, ESA Special Publications. European Space Agency, ESA.

Acknowledgements

First of all I would like to thank my supervisor Peter Bauer-Gottwein. You have been support and inspiration during the last years with an always open door and mind. My co-supervisor Henrik Madsen, you were a very thoughtful help throughout my studies. Thank you.

I am grateful for the cooperation with DHI throughout this PhD project. Besides Henrik Madsen, especially Peter Nygaard Godiksen and Marc-Etienne Ridler: Many thanks for a fruitful cooperation and for sticking with me also through difficult times while working on the data assimilation framework.

DHI Italy, the Interregional Agency for the Po River (AIPo) and ICIMOD are acknowledged for providing data for the Po and Brahmaputra rivers. Funding provided by the LOTUS and CRUCIAL projects is gracefully acknowledged.

LOTUS involved working together with Per Knudsen, Ole B. Andersen, Karina Nielsen, and Heidi Villadsen, all from the National Space Institute at DTU. Thanks for a very enjoyable collaboration and for helping me understanding the technical details of satellite altimetry. Moreover, thanks to the other collaborators involved in the two projects from Newcastle University, CLS, Toulouse, and Starlab, Barcelona.

I spent two great months with the Hydrology group of the Research Institute for Geo-Hydrological Protection (CNR IRPI) in Perugia, Italy. Thank you everybody there, you welcomed me warmly, and special thanks to Angelica Tarpanelli.

Thanks to my colleagues from DTU Environment for making this a great place to work. I want to mention the administrative and IT staff, who are extremely helpful and important for the entire department. You are treasured!

I sincerely enjoyed working with all of you on the border between hydrology and remote sensing. I hope to see you and work with you again in the future!

To all my friends from DTU and outside of it who made the last three years a nice ride… I do not want to list names (and then forget someone). But you know who you are: Thank you! And last, but not least: A big thank you to my family and Pernille.

Summary

The global coverage of in situ observations of surface water dynamics is insufficient to effectively manage water resources. Moreover, the availability of these data is decreasing, due to the lack of gauging stations and data sharing. Satellite radar altimetry, initially developed to monitor ocean water levels, also offers measurements of water levels of rivers and lakes on a global scale. Because of the continuous upstart of new missions, and sensor and processing innovations, the importance of satellite altimetry data for the hydrologic community is increasing.

CryoSat-2, launched by the European Space Agency (ESA) in 2010, is one of the more recent additions to the set of satellite altimeters. It is unique due to two characteristics. First, its radar altimetry instrument provides, besides conventional observations in Low Resolution mode (LRM), observations in Synthetic Aperture Radar (SAR) and Synthetic Aperture Radar Interferometric (SARIn) mode. SAR and SARIn have reduced footprint size in the along-track direction owing to delay/Doppler processing, potentially increasing observation accuracy. Second, CryoSat-2 is placed on a unique long-repeat orbit with a cycle of 369 days. This is different from previous and current satellite altimetry missions, which are in short-repeat orbits with cycles of 10 to 35 days.

The orbit configuration of CryoSat-2 is a challenge for hydrologic applications. Short-repeat missions allow deriving time series at locations where the satellite ground track repeatedly intersects with the river – the so-called virtual stations. Because of the long repeat cycle of CryoSat-2, its virtual station time series have a temporal resolution of 369 days, which is inadequate for most hydrologic applications. This requires rethinking some methods to process such data, distribute them to the hydrologic community and combine them with river models. However, the orbit configuration of CryoSat-2 also results in a small inter-track distance, providing measurements with unprecedented spatial resolution along rivers. These points were the main motivation for this PhD study.

Two case studies were chosen; the Po River in Italy, and the Brahmaputra River in South Asia. CryoSat-2 level 2 data, i.e. point observations of surface height, were filtered over high resolution river masks derived from Landsat imagery. This yielded roughly 340 observations per year over the Po River, and roughly 1300 per year over the Brahmaputra River. The CryoSat-2

observations were validated against in situ observations along the Po River. The average root mean square error (RMSE) between CryoSat-2 and in situ observations was found to be 0.38 m, which is comparable to previous missions.

The CryoSat-2 water level observations then were used to parameterize 1-dimensional (1D) hydrodynamic river models. For the Po River, where surveyed cross sections are available, CryoSat-2 was used to calibrate channel roughness. The distributed CryoSat-2 data allowed calibrating channel roughness with a higher spatial resolution than possible in a conventional approach using in situ data. Over the ungauged Brahmaputra River, CryoSat-2 data were used to calibrate shapes of synthetic cross sections. For the calibrated model, the RMSE between simulated and CryoSat-2 observed water levels is 1.24 m. It is assumed to accurately reproduce water level-discharge relationships; without relying on river cross section information.

Finally, the potential of CryoSat-2 data for updating hydrodynamic models was evaluated based on the Brahmaputra River case study. A flexible Data Assimilation (DA) framework was developed, which can assimilate observations of river state with any spatio-temporal resolution to a DHI MIKE HYDRO River 1D hydrodynamic model. DA can, amongst others, improve flood forecasting. Synthetic tests showed a high potential of CryoSat-2, improving discharge predictions of the model in terms of Continuous Ranked Probability Score (CRPS) by up to 32 %, while real tests could improve the CRPS by up to 10 %. Also, synthetic experiments were conducted to evaluate the impact of increased observation accuracy and different sampling patterns.

The results from this study highlight the value of CryoSat-2 altimetry data, which delivers water level observations with unprecedented spatial resolution along rivers. The study presented methods to cope with the distinct spatio-temporal distribution of the CryoSat-2 data and move beyond the common concept of virtual stations. Potentially, this flexibility opens up new opportunities for the use of remote sensing data in the hydrologic community.

Dansk sammenfatning

Der findes, på globalt plan, ikke tilstrækkelige observationer af overfladevand og deres dynamikker til at kunne forvalte vandressourcerne. Samtidig er tilgængeligheden af data faldende, grundet manglende in-situ observationer og deling af eksisterende data. Satellitbaseret radarhøjdemåling, som oprindelig blev udviklet til at overvåge havvandstande, muliggør observationer af vandstande i floder og søer på et globalt plan. Da der fortsat igangsættes nye satellitmissioner og udvikles sensorer og databehandlingsmetoder er relevansen af satellithøjdemåling for det hydrologiske miljø stigende.

CryoSat-2, som blev opsendt af det europæiske rumagentur (ESA) i 2010, er en af de nyere satellithøjdemålere. CryoSat-2 er unikt på to punkter. For det første kan højdemåleren, udover den konventionelle Low Resolution mode (LRM), opereres i Synthetic Aperture Radar (SAR) og Synthetic Aperture Radar Interferometric (SARIn) mode. Her opnås et reduceret footprint i "along track" retningen ved hjælp af Doppler processering, som potentielt øger observationers nøjagtighed. For det andet bevæger CryoSat-2 sig i et kredsløb med en lang cyklus på 369 dage. Kredsløbet er derved forskelligt fra andre satellitter, hvis kredsløb har kortere cykler på mellem 10 og 35 dage.

Det er i særdeleshed kredsløbsmønsteret, der giver en udfordring for anvendeligheden af CryoSat-2 data indenfor hydrologi. Kredsløb med kort cykler gør det muligt at udlede tidsserier på lokaliteter hvor satellittens jordbane krydser en flod gentagne gange (også kaldet virtuelle målestationer). På grund af CryoSat-2s lange cyklus har virtuelle målestationer en tidsopløsning på 369 dage, som er utilstrækkelig i de fleste hydrologiske sammenhænge. Der er derfor brug for nytænkning af databehandlingsmetoder for at gøre CryoSat-2 brugbar indenfor hydrologi og især til anvendelse i flodmodellering.

Der er valgt to casestudier: Po floden i Italien og Brahmaputra floden i Sydasien. CryoSat-2 level 2 data, det vil sige punktobservationer af overfladehøjder, blev filtreret over højopløselige flodmasker fra Landsat-billeder. Dette resulterede i omtrent 340 observationer per år for Po floden og omtrent 1300 observationer per år for Brahmaputra floden. For Po floden blev CryoSat-2 observationerne valideret med in situ observationer. Den gennemsnitlige root mean square error (RMSE) mellem CryoSat-2 og in situ

observationer var på 0,38 meter, hvilket er sammenligneligt med tidligere satellitmissioner.

CryoSat-2 vandstandsobservationer blev herefter anvendt til at parametrisere en éndimensionel (1D) hydrodynamisk flodmodel. For Po floden, hvor opmålte tværsnit af flodlejet er tilgængelige, blev CryoSat-2 brugt til at kalibrere ruheden af flodlejet. Idet CryoSat-2 data er rumligt fordelt, var det muligt at kalibrere modellen med en højere rumlig opløsnings af flodlejets ruhed end med traditionelle in situ data. For Brahmaputra floden blev CryoSat-2 anvendt til at kalibrere datum og udformningen af syntetiske flodlejetværsnit. Med den kalibrerede model opnås en RMSE mellem observeret og simuleret CryoSat-2 vandstande på 1,24 meter. Modellen reproducerer forholdet mellem afstrømning og vandstand tilfredsstillende; uden brug af information om tværsnit af flodlejet.

Endeligt blev potentialet for anvendelse af CryoSat-2 data til at opdatere hydrodynamiske modeller undersøgt med Brahmaputra floden som eksempel. En fleksibel data assimilering (DA) opsætning blev udviklet til at kunne assimilere data med enhver tids- og rumligopløsning med en DHI MIKE HYDRO River 1D hydrodynamisk model. DA har potentiale til at forbedre forvarslinger om oversvømmelser. Syntetiske forsøg viste et højt potentiale ved at forbedre modellerede afstrøms-prædiktioner, udtrykt ved en forbedring af Continuous Ranked Probability Score (CRPS) med op til 32 procent. Forsøg med faktiske data viste en tilsvarende forbedring på 10 procent. Derudover blev det undersøgt i hvilket omfang DA ydeevne påvirkes af øget observationsnøjagtighed og varierende observationsmønstre.

Resultaterne fra dette arbejde fremhæver værdien af CryoSat-2 vandstandsmålinger, som tilvejebringer observationer af vandstand i floder med hidtil uset høj rumlig opløsning. Arbejdet præsenterer metoder til at håndtere den særegne tidslige og rumlige opløsning af CryoSat-2 data og anvender succesfyldt data hinsides de konventionelle virtuelle målestationer. Denne fleksibilitet åbner for nye muligheder for anvendelse af telemåling i hydrologi, som hidtil ikke har været muligt.

Table of contents

Abbreviations

1D	1-dimensional
AR(1)	First-order autoregressive model
CI	Confidence interval
CRPS	Continuous Ranked Probability Score
DA	Data Assimilation
DEM	Digital elevation model
EnKF	Ensemble Kalman Filter
ESA	European Space Agency
ETKF	Ensemble Transform Kalman Filter
HT	Hidden truth
KF	Kalman Filter
LRM	Low resolution mode of CryoSat-2
ME	Mean error
NDVI	Normalized Difference Vegetation Index
NIR	Near-infrared
NSE	Nash-Sutcliffe model efficiency
RMSE	Root mean square error
SAR	Synthetic Aperture Radar mode of CryoSat-2; not to be confused with Synthetic Aperture Radar (SAR) imagery
SARIn	Synthetic Aperture Radar Interferometric mode of CryoSat-2
SRTM	Shuttle Radar Topography Mission

1 Introduction

Surface waters are a source of drinking water for many people globally. Additionally, rivers, lakes, reservoirs, wetlands etc. serve agricultural and industrial water uses, including electricity generated by hydropower. However, the same water bodies commonly also pose a risk to the people inhabiting their banks through flooding (Loucks and van Beek, 2005). These issues, like flood hazards and sufficient supply of clean water, are further exacerbated by population growth and climate change (Arnell and Gosling, 2016; Vörösmarty et al., 2000). Besides the direct links to the anthroposphere, rivers, lakes and wetlands also support diverse ecosystems.

To describe, monitor, and model water systems, knowledge of quantity and dynamics of surface water flows and storage is needed. Essential parameters in this context are, for example, surface water area and surface water elevation, and their variability in space and time. On the global scale, the spatial coverage of in situ observations is generally considered insufficient (World Water Assessment Programme, 2009). Nonetheless, the availability of in situ stage data of rivers is decreasing across the globe (Calmant and Seyler, 2006). Reasons for this are the lack of gauging stations, and also political decisions to not share data (Brakenridge et al., 2012). Surface water extent and elevation can be remotely sensed with generally increasing accuracy and spatio-temporal resolution. Other variables of the hydrologic cycle can also be remotely sensed, e.g. precipitation, temperature, evapotranspiration, total water storage, snow cover, or soil moisture. All these observations aid process understanding, monitoring, or inform hydrological models. They are needed to answer questions concerning the global water and energy cycles, observe flow hydraulics and solve issues of water resource management (Alsdorf et al., 2007). Lettenmaier et al. (2015) provide an overview of current applications and limitations of such observations. Despite the emergence of new technologies such as Unmanned Aerial Vehicles and trends such as miniaturization of sensors (McCabe et al., 2017), satellite missions of agencies such as NASA and ESA remain central to global Earth observation.

Observations of water levels can be obtained from satellite radar altimeters. A radar altimeter measures the surface elevation by sending out a microwave pulse and recording its echo. Most of these missions were initially developed to monitor water levels in oceans. However, they also proved useful over inland water bodies (Alsdorf et al., 2007; Berry and Benveniste, 2010; Calmant et al., 2009). They provide the potential for global water level measurements,

and supplement or replace in situ observations. Such measurements are used today to monitor river and lake water levels and storage, aid discharge estimation in rivers, and to inform and update river models (Calmant et al., 2009), despite limitations owing to observation uncertainty, spatio-temporal resolution and target size.

Most current and past satellite altimetry missions have orbit configurations with short repeat cycles between 10 and 35 days. This allows deriving time series of water level observations with said temporal resolution at so-called virtual stations where the ground track intersects with the water body (Rosmorduc et al., 2011). The spacing between the ground tracks is between 80 and 315 km at the equator.

The ESA mission CryoSat-2, launched in 2010 with the primary objective to observe ice shields and sea ice, has an unconventional orbit configuration with a long repeat cycle of 369 days (European Space Agency and Mullard Space Science Laboratory, 2012; Wingham et al., 2006). The resulting drifting ground track pattern poses challenges to data users from the hydrologic community: Many of the developed methods for processing satellite radar altimetry and providing it to the hydrologic community, as well as its combination with hydrologic models were tailored to orbit configurations with short repeat cycles and the virtual station time series. It is not possible to directly derive meaningful water level time series at virtual stations from CryoSat-2.

This PhD study focused on the evaluation of CryoSat-2 altimetry data over rivers, and their usefulness to inform and update large-scale hydrodynamic river models. Special attention was given to the challenges and advantages that arise from the unique orbit configuration of CryoSat-2. The main objectives of the research were:

- Evaluation of multi-mode CryoSat-2 altimetry data over rivers (Paper II)
- Exploiting the unique spatio-temporal sampling pattern of CryoSat-2 for the parameterization of hydrodynamic river models (Paper II and Paper III)
- Development of a flexible data assimilation framework that allows updating hydrodynamic river models with CryoSat-2 data, and data with any spatio-temporal distribution (Paper IV)

Paper I reviews the use of CryoSat-2 altimetry data over rivers and lakes, and puts CryoSat-2 and its unique orbit configuration into perspective with other satellite altimetry missions.

This synopsis summarizes the work conducted during the PhD study. A brief introduction to satellite altimetry is given in section 2. An overview of the CryoSat-2 mission and its particularities which are a focus of this study are presented in section 3. Based on this, section 4 provides the general context of the research and its objectives. Section 5 briefly introduces the two case studies. Sections 6 to 8 present the main methods and findings from this study, divided into the three main objectives. Finally, sections 9 and 10 close with concluding remarks and future perspectives of the research conducted. The four papers that were written as part of this PhD study and are referenced throughout the thesis can be found in the appendix.

2 Principles of satellite radar altimetry

Satellite radar altimeters are used to observe surface heights from space, for example of oceans, ice, and inland water. A radar altimeter emits a short radar pulse at nadir direction and records its echo reflected from the surface of the Earth. Knowing the travel time of the echo it is possible to calculate the range, i.e. the distance between satellite and surface (Figure 1) using the speed of the signal. Theoretically, electromagnetic waves propagate at the speed of light, but the atmosphere slows down the signal slightly. Atmospheric propagation corrections are applied to account for this. Knowing the precise position and orientation of the satellite, the surface height above a reference ellipsoid and finally a geoid can be determined. Besides this, geophysical corrections have to be applied to account for ocean and solid Earth tides and effects of variable load on the surface.

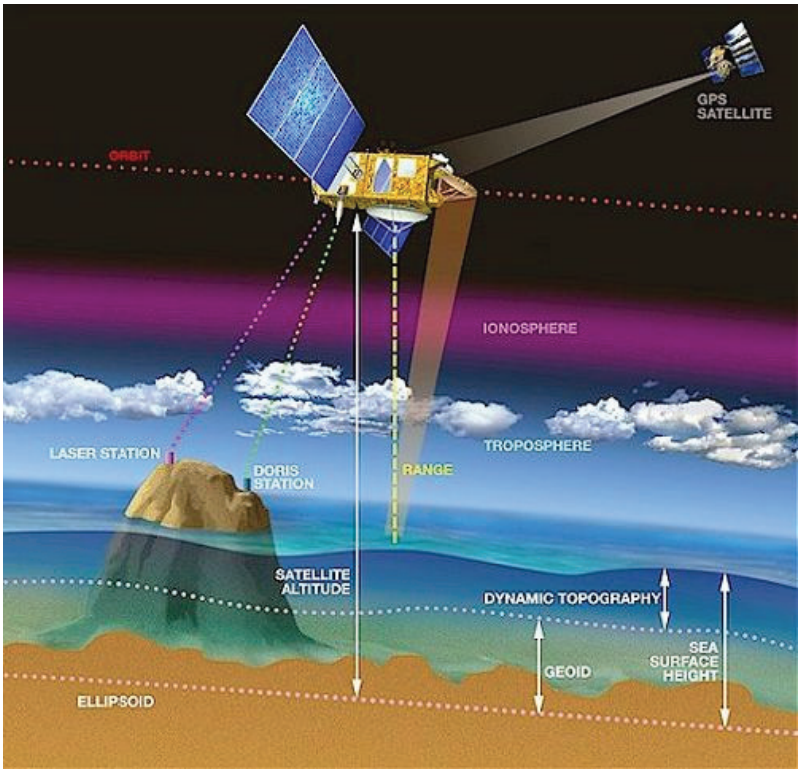

Figure 1. The principle of satellite radar altimetry. From Rosmorduc et al. (2011).

A crucial step in determining surface height from a radar altimeter is the interpretation of the echo. The intensity of the echo of each pulse is recorded over time. To reduce noise, it is common to average the signal over a series of pulses, which are sent out with high pulse repetition frequency (in the range of kHz). The resulting signal is referred to as waveform, or as level 1b data. In the waveform, the leading edge has to be found. The leading edge is assumed to represent the reflection from the surface of interest. Usually, tracking of the leading edge is performed continuously on board of the altimeter. This is necessary to keep the narrow so-called range window where the altimeter is sensitive to the signal in the correct time period. For more precise determination of the surface elevation, a sophisticated analysis of the waveform is performed on ground. This process is called retracking and ultimately outputs observed surface heights, which are referred to as level 2 data. Level 2 data come in the form of point data along the nadir of the satellite, with the coordinates, a time stamp, the observed surface height and often more metadata.

Over homogenous surfaces such as the open ocean or large lakes, the waveforms expose a well behaved "ocean-like" shape. This allows matching simulated waveforms from physical models to the observed ones and obtaining very precise estimates of water surface elevation with accuracies in the range of few centimetres. Over more heterogeneous surfaces, such as most inland water targets, the waveforms have less regular and predictable shapes. This is related to, amongst others, the footprint sizes of conventional radar altimeter instruments, which are roughly circular with a diameter in the range of a few kilometres. Consequently, waveforms over small inland water bodies are contaminated by the surrounding land surfaces. Retracking over inland waters often is performed by empirical retrackers. Because the water surface frequently represents the brightest target for the radar altimeter within the footprint (Berry et al., 2005), water bodies smaller than the footprint still can be observed.

For a general introduction to satellite radar altimetry and its monitoring applications the reader is referred to Chelton et al., 2001 or Rosmorduc et al., 2011. Calmant et al., 2016 provide a similar introduction focussed on inland water bodies.

3 CryoSat-2 mission overview

The European Space Agency (ESA) CryoSat-2 satellite was launched in April 2010. Its main objectives are the monitoring of sea ice and terrestrial ice sheets. Like many other satellite altimetry missions it, however, also proved useful over inland water bodies (Paper I). The CryoSat-2 mission is unique due to two features, which are among the main motivations to study it in the framework of this PhD project.

First, the altimeter instrument on CryoSat-2, called SIRAL (Synthetic Aperture Interferometric Radar Altimeter) is operated in three distinct modes: Low Resolution (LRM), Synthetic Aperture Radar (SAR), and Synthetic Aperture Radar Interferometric (SARIn) mode; the latter two being novel and unique to CryoSat-2[1]. LRM operates like a conventional, pulse-limited radar altimeter in a similar manner as for example the RA-2 instrument on Envisat with a roughly circular footprint. In case of CryoSat-2 the footprint diameter is about 1.65 km over smooth surfaces and considerably larger over rough surfaces. An increase of footprint size with surface roughness is a general characteristic of radar altimeters (Chelton et al., 2001). For SAR and SARIn, delay/Doppler processing (first suggested by Raney, 1998) increases the along-track resolution to approximately 300 m. SARIn mode additionally employs a second antenna which allows determining the off-nadir location of the dominant echo within the footprint.

Basically, SAR mode is applied over areas with sea ice and some coastal zones. SARIn mode is applied over the topographic ice sheet margins and glaciers, and also over some river systems. LRM data are available everywhere else. The mask determining the global distribution of the three modes (Figure 2) was adapted repeatedly during the CryoSat-2 mission.

[1]Sentinel-3A (launched in 2016), Sentinel-3B (launch planned for 2018), and Jason-CS/Sentinel 6 (launch planned for 2020) also carry radar altimeters capable of operating in LRM and SAR mode, but not in SARIn.

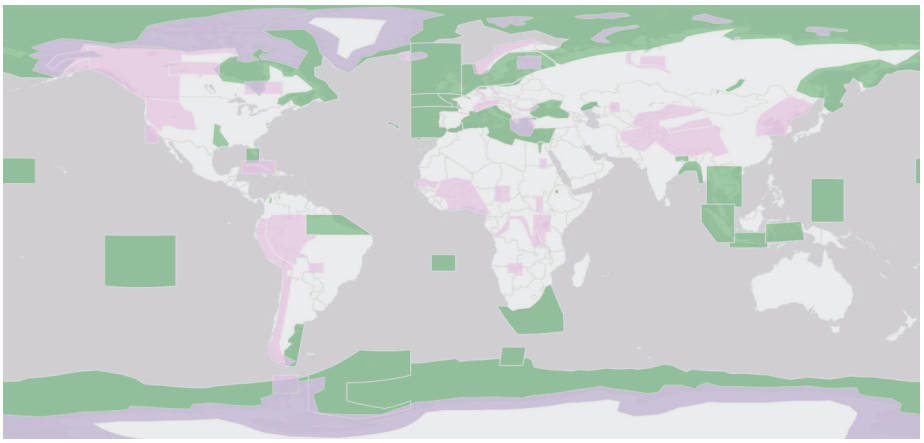

Figure 2. CryoSat-2 mode mask v3.9 (available at https://earth.esa.int/web/guest/-/geographical-mode-mask-7107). Green: SAR mode. Purple: SARIn mode. All remaining areas: LRM mode.

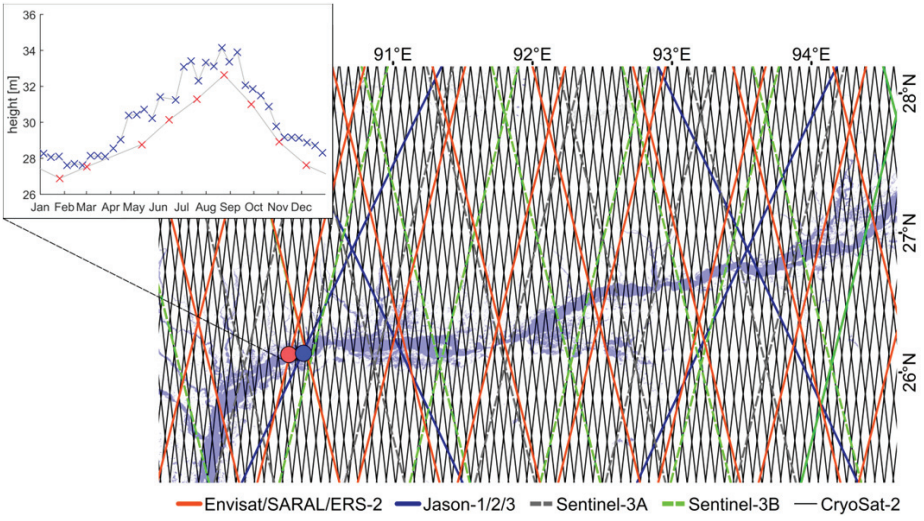

Figure 3. Ground tracks from different satellite altimetry missions over the Brahmaputra River. The repeat cycle is 35 days for Envisat/SARAL/ERS-2, 10 days for Jason-1/2/3, 27 days for Sentinel-3A/B, and 369 days for CryoSat-2. The two dots are Envisat and Jason-2 example virtual stations. Their observed water levels in 2009 are shown in the inlet; data from DAHITI (Schwatke et al., 2015).

Second is the long-repeat orbit of CryoSat-2 with a full repeat cycle of 369 days (and 30 day subcycles), which maybe has the biggest impact on its application over inland water bodies. All previous radar altimetry missions have been on short-repeat orbits with repeat cycles between 10 and 35 days (Table 1). At intersections of the ground track with a water body like the Brahmaputra River shown in Figure 3, this allows deriving water level time series at virtual stations. The concept of virtual stations simplifies processing of the altimetry data and their combination with models as will be further detailed in the following section. For CryoSat-2, adaptation of some common methods for working with satellite altimetry over rivers is needed. The orbit configuration of CryoSat-2, however, also leads to a small inter-track distance, which can be seen as one of its main advantages over previous missions. This is one of the main themes of this PhD study.

Further information about the CryoSat-2 mission is presented in Paper I. Details are described by Wingham et al. (2006) or can be found in the CryoSat Product Handbook (European Space Agency and Mullard Space Science Laboratory, 2012).

4 Satellite altimetry over inland waters

4.1 Availability for hydrologic applications

Table 1 lists past, current and planned satellite altimetry missions with relevance for inland waters and some of their key characteristics.

Table 1. Overview of past, current, and planned satellite altimetry missions with relevance for inland waters (adapted from Paper I).

Satellite	Altimeter instrument	Mission period	Repeat cycle [d]	Equatorial inter-track distance [km]
TOPEX/Poseidon	TOPEX/Poseidon	1992 – 2005	10	315
ERS-2	RA	1995 – 2011	35	80
Jason-1	Poseidon-2	2001 – 2013	10	315
Envisat	RA-2	2002 – 2012	35	80
ICESat*	GLAS	2003 – 2010	91	30
OSTM/Jason-2	Poseidon-3	2008 – present	10	315
CryoSat-2	SIRAL	2010 – present	369	7.5
SARAL	AltiKa	2013 – present	35	80
Jason-3	Poseidon-3B	2016 – present	10	315
Sentinel-3A	SRAL	2016 – present	27	104
Sentinel-3B	SRAL	launch planned 2018	27	104
ICESat-2*	ATLAS/MABEL	launch planned 2018	91	30
Jason-CS/Sentinel-6	Poseidon-4	launch planned 2020	10	315
SWOT**	KaRIn	launch planned 2021	21	

*ICESat and ICESat-2 use a lidar altimeter instrument instead of radar altimeters like the other listed missions. ICESat-2 will use a multi-beam setup, effectively reducing the inter-track distance (Markus et al., 2017)
**SWOT with the KaRIn instrument is a radar interferometer instead of nadir altimeters as on the other listed missions: it delivers surface elevation imaging of 93 % of the surface of the Earth between 78ºS and 78ºN (Biancamaria et al., 2016)

Hydrologists rarely perform the altimetry raw data processing and retracking themselves. They rely on the availability of level 2 or level 3 data, i.e. observed surface heights or aggregated time series of those. The data can be obtained for example directly from the agencies, in the case of CryoSat-2 from ESA (https://earth.esa.int/web/guest/-/how-to-access-cryosat-data-6842). Their level 2 products, however, often are not optimized for the use over inland water bodies, because the main purpose of the missions is the ob-

servation of sea surface heights or ice. Hence, there exist several databases providing level 3 data specifically over inland water bodies, applying tailored processing:

- DAHITI (http://dahiti.dgfi.tum.de/en/) providing virtual station time series from multiple missions over many large rivers and some lakes
- HydroWeb (http://www.legos.obs-mip.fr/en/soa/hydrologie/hydroweb/), similar to DAHITI
- River and Lake (http://tethys.eaprs.cse.dmu.ac.uk/RiverLake/shared/main) also similar to the above, but discontinued in 2014
- HydroSat (http://hydrosat.gis.uni-stuttgart.de/php/index.php) providing water level time series from satellite altimetry over some rivers along with other remotely sensed or derived variables (such as surface water extent, discharge)

And two databases providing water levels over lakes only:

- AltWater (http://altwater.dtu.space/) providing water level time series from CryoSat-2 over a series of lakes
- G-REALM (https://www.pecad.fas.usda.gov/cropexplorer/global_reservoir/) providing water level time series from multiple missions over lakes and reservoirs

Many of the processing methods for inland water satellite altimetry have been tailored to virtual station time series: HydroWeb, for example, uses rectangular masks at the locations of the virtual stations to filter data (Rosmorduc, 2016), and not continuous river masks as would be needed for CryoSat-2 with its drifting ground track. DAHITI applies a river mask via a latitude threshold (as ground tracks generally run in a predominantly northerly-southerly direction). Also, the mentioned sources provide their river data in form of virtual station time series; the distribution format would have to be adapted for CryoSat-2. These challenges are the likely reasons why CryoSat-2 data is missing in most of the databases listed above.

Accuracy of water level observations is in the range of few centimetres for lakes and in the range of few decimetres for rivers (an overview of selected altimetry studies with validation results is provided by Villadsen et al., 2016 or O'Loughlin et al., 2016). Accuracy depends – besides differences between missions and differences between retracking algorithms – on the size of the

water target. The current minimum river width for radar altimetry observations is one hundred to a few hundred metres (Biancamaria et al., 2017; Maillard et al., 2015). Also the surrounding topography has an influence: In steep terrain, an altimeter may struggle to keep its narrow range window where it is sensitive to observations close to ground level (Dehecq et al., 2013). This is the case if the altimeter is, like on CryoSat-2, operating a closed-loop control to adapt the position of the range window using on-board tracking instead of an open-loop control where the range window follows a predefined digital elevation model (DEM).

4.2 Monitoring of rivers and lakes

Satellite altimetry datasets can be used to monitor water levels in rivers and lakes. This is especially attractive over regions that are sparsely monitored on the ground. Monitoring of lake levels, and sometimes the related water storage, is widespread (e.g. Baup et al., 2014; Gao, 2015; Tourian et al., 2015), also using data from CryoSat-2 (e.g. Jiang et al., 2017; Kleinherenbrink et al., 2015; Song et al., 2015).

The focus of this study is the use of satellite radar altimetry over rivers, where monitoring mainly is performed over large rivers: The Amazon Basin is a popular target, where for example Santos da Silva et al. (2010) derived water levels from Envisat and ERS-2 with an accuracy of approximately 40 cm compared to in situ water level data. Over the largely ungauged Congo Basin, Envisat altimetry data were used to characterise the water level variations in nine hydrologically similar subcatchments (Becker et al., 2014). A combination of Envisat altimetry data, a global inundation extent product, and GRACE gravimetry for total water storage was used over the water-stressed Ganges-Brahmaputra Basin to estimate surface water storage and subsurface storage variations (Papa et al., 2015). These are just few examples of many; other studies include Frappart et al. (2006) or Hall et al. (2012) over the Amazon River, Jarihani et al. (2013) over different Australian water bodies, or Lee et al. (2015) over the Congo Basin.

The application of CryoSat-2 altimetry over rivers is still limited, most likely due to the mentioned challenges arising from its drifting ground track pattern.

4.3 Merging and densification of altimetry data

The typical spatio-temporal resolution of single mission altimetry data along river networks is poor when directly used for flood forecasting or similar purposes. In an effort to resolve this, methods to merge data from multiple

missions along river networks have been developed, which use distant observations to create data with higher temporal resolution than originally available from the satellite instruments. Tourian et al. (2016) combined data from multiple short-repeat missions. Their method transfers altimetry measurements along the river network accounting for travel time using a quantile approach, which exploits the existence of virtual station time series. Thus, it is not straight-forward to integrate CryoSat-2 with its drifting ground track into their method.

There also exist methods for spatio-temporal interpolation along river networks. In theory such methods could provide water level (or derived discharge) along a river network continuously in time and space; something that usually is derived from a hydrologic model, and not observations only. Meaningful interpolation of point-based observations has to take into account the changing variability of water levels along the river network in space and time, i.e. some variants of spatio-temporal kriging are applied (e.g. Skøien and Blöschl (2007)). In the context of river altimetry, Boergens et al. (2016) used a spatio-temporal kriging approach to link multi-mission virtual station data along the Mekong River. Their covariance model, which describes the variability of water levels in time and space, requires observations in the form of virtual station data, which makes it unsuitable for the distributed CryoSat-2 data. A more flexible river kriging method was developed by Paiva et al. (2015), in preparation for data from the upcoming Surface Water and Ocean Topography (SWOT) mission.

Over rivers, observed water levels are often used to derive further variables of interest, such as river discharge or hydraulic parameters of the river channel. Also, the observations can inform river models or update them with the aim of improving model forecasts of discharge, water level, and water extent (sections 4.4 through 4.6).

4.4 Deriving discharge from altimetry data

Estimation of river discharge from satellite altimetry is usually performed in combination with auxiliary data such as remotely sensed water extent or in situ water level-discharge relationships. Birkinshaw et al. (2014) used a combination of water level and slope from ERS-2 and Envisat altimetry and river width from Landsat imagery as input to an empirical equation to estimate discharge (Bjerklie et al., 2003). Their derived daily discharge shows a good Nash-Sutcliffe efficiency (NSE) of 0.86 to 0.90 compared to in situ measurements. Using Envisat altimetry data combined with MODIS near-infrared

(NIR) imagery as a proxy for river flow velocity, Tarpanelli et al. (2015) estimated discharge with a root mean square error (RMSE) of about 37 % over the Po River, Italy. A similar approach, using MODIS NIR imagery to estimate river widths over eight major river basins was used by Sichangi et al. (2016). They also provide an overview of studies estimating river discharge from different remote sensing data, some without altimetry data. Trying to handle the poor temporal resolution of satellite altimetry for discharge estimates, Tourian et al. (2017) used multi-mission altimetry from Envisat, SARAL/AltiKa and Jason-2 over the Niger Basin. After densifying the altimetry data as mentioned in the previous section (Tourian et al., 2016), a stochastic model was used to estimate discharge from the available water levels.

4.5 Parameterization of rivers and river models

Despite their limited spatio-temporal resolution and accuracy, water levels from satellite altimeters have been used successfully for the hydraulic characterization of rivers and the parameterization of river models. For example, Envisat virtual station altimetry data have been used to calibrate parameters of a hydrologic model of a subcatchment of the Amazon River (Getirana, 2010). TOPEX/Poseidon data aided the parameterization of cross section depth and channel roughness of a 1D-2D model of the ungauged Ob River in Siberia (Biancamaria et al., 2009). Similarly, Domeneghetti et al. (2014) evaluated the usefulness of ERS-2 and Envisat data over a model of the Po River to calibrate channel roughness. A hydrologic model was calibrated with the help of TOPEX/Poseidon altimetry data over the Mississippi River (Sun et al., 2012).

A notable exception to the use of virtual station altimetry is the use of ICESat altimetry. ICESat carries a lidar altimeter (Schutz et al., 2005), and its inland water data has been made available by O'Loughlin et al. (2016). With a repeat cycle of 91 days, it has an orbit configuration in between the short-repeat missions with virtual station data and the long-repeat mission CryoSat-2 with its drifting ground track. It features a relatively small inter-track distance which was used by O'Loughlin et al. (2013) to derive water level profiles along the Congo River during different flow regimes and other hydraulic parameters such as the length of backwater effects. The potential of water level observations with high spatial resolution is also pointed out by Garambois et al. (2016): If a river flows along the satellite ground track, any mission can observe river water level profiles. They exploit this over a tributary of the

Amazon River with Envisat, and derive various hydraulic characteristics of the river.

Generally, the hydrologic community has high expectations for the upcoming SWOT mission to be launched in 2021. The main innovation of SWOT is that it will deliver surface elevation information along two 50 km wide swaths, instead of point observations along nadir only. Moreover, it will simultaneously deliver observations of water level slope and water extent. There is a large number of studies that estimate river discharge (Durand et al., 2014; Gleason and Smith, 2014, etc.; an overview is provided by Biancamaria et al., 2016), or derive hydraulic parameters of rivers (Garambois and Monnier, 2015; Mersel et al., 2013) based on synthetic SWOT data.

The higher spatial resolution of CryoSat-2 altimetry data along rivers is exploited for model parameterization in both Paper II and Paper III, showing that even for a well monitored river CryoSat-2 can deliver additional information.

4.6 Updating of river models

Finally, remote sensing data can also be used to directly update states or parameters of hydraulic or hydrologic models. This is referred to as data assimilation (DA). Different parts of hydrologic-hydraulic models are updated using various remotely sensed information. For example, observations of soil moisture have been used successfully to update hydrologic models. Also, observations of flood extent, total water storage, snow coverage, or land surface temperature can be used to improve predictions from hydrologic or land surface models. Liu et al. (2012) provide an overview.

In the context of satellite altimetry data, DA was performed extensively with the above mentioned synthetic SWOT data (an overview is provided by Biancamaria et al., 2016). There also have been several studies working with real data from past and current altimetry missions, and their virtual station time series. Michailovsky et al. (2013) assimilated Envisat altimetry data to a model of the Brahmaputra River, updating the state of the Muskingum routing scheme. Similarly, Envisat altimetry data were used to update a 1D hydrodynamic model of the Amazon river basin (Paiva et al., 2013). Jason-2 altimetry data are used in an operational system to improve flood forecasting in the Ganges-Brahmaputra-Meghna Delta in Bangladesh (Hossain et al., 2014).

Common to the mentioned studies using data from past and current altimetry missions is that they, in one way or the other, are limited to be used with altimetry data in the form of virtual station altimetry. So far, no assimilation studies have been performed with distributed data like provided by CryoSat-2 (only synthetic studies with SWOT data have been performed). This will be further discussed in section 8: as part of this PhD study, a DA framework was developed and tested with CryoSat-2 data (Paper IV).

5 Case studies

Figure 4 shows the two case studies used in this PhD study, the Po River in Italy, and the Brahmaputra River in South Asia.

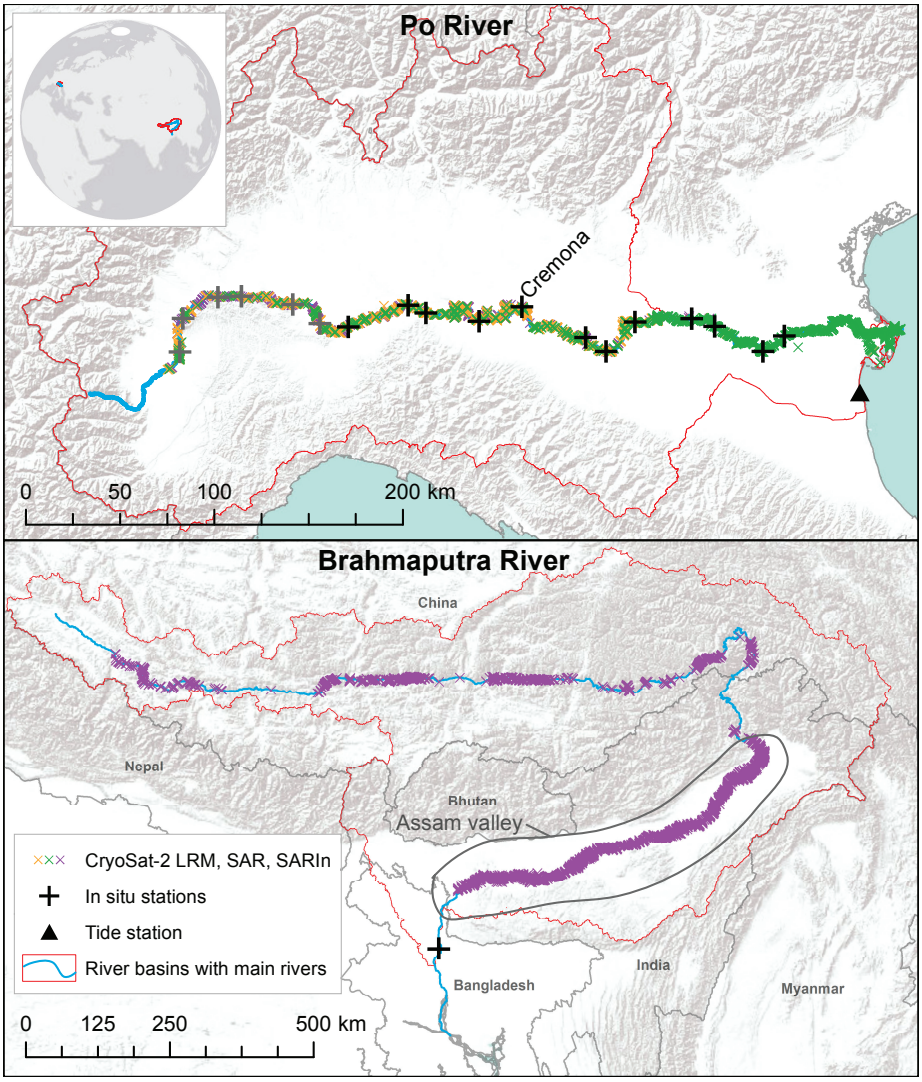

Figure 4. The Po River and Brahmaputra River case studies. The available CryoSat-2 data are displayed, after filtering over river masks and outlier removal.

The 652 km long Po River in Northern Italy drains a catchment area of about 71 000 km^2. The average discharge close to its outlet is 1470 $m^3 s^{-1}$ and it exhibits two high-flow periods: one in spring and one in autumn (Montanari, 2012). It is mostly a single-channel river with river widths reaching up to about 500 m. The Po River is well monitored; hence it was used to evaluate the observation uncertainty of CryoSat-2 water level observations against in situ data from 18 stations along the river. Channel roughness calibration was performed in a 1D hydrodynamic model of the Po River (both Paper II).

Data availability for the Brahmaputra River, on the other hand, is limited. The Brahmaputra River flows from the Tibetan plateau in China through the Himalayan mountain range into India, and finally merges in Bangladesh into the Ganges-Brahmaputra-Meghna Delta. Its catchment size is approximately 580 000 km^2 and the main river has a length of around 3000 km. After it leaves the Himalayas, the river flows through the Assam valley in India as a multi-channelled braided river. Here, the total width of the river bed can reach more than 10 km, with single channels of up to 1 km. Average discharge is close to 20 000 $m^3 s^{-1}$, with a distinct flood season in summer due to snowmelt (early summer) and monsoon rain (late summer) (Jain et al., 2007). The river is monitored by India and China; however, most hydrologic data are unavailable to the public. This is particularly relevant for Bangladesh which is regularly hit by severe floods (Biancamaria et al., 2011b) and could benefit from additional information about its state. CryoSat-2 data were used to estimate cross section shapes in a 1D hydrodynamic model (Paper III), and finally to update the states of a river model via assimilating the altimetry data along the Assam valley (Paper IV).

6 Processing and validation of CryoSat-2 altimetry data over rivers

6.1 CryoSat-2 altimetry data

CryoSat-2 level 2 altimetry data were used in this study. The data were provided by the National Space Institute, Technical University of Denmark (DTU Space). They are based on the ESA level 1b 20 Hz product, and retracked using an empirical Narrow Primary Peak Retracker (NPPR) (Jain et al., 2015). This is assumed to be the best suited retracker for rivers, according to an analysis by Villadsen et al. (2016).

Over the Po River, CryoSat-2 data were evaluated from the beginning of the mission in 2010 until 2016. In the Brahmaputra River case study, data from 2010 until 2013 (for cross section calibration, section 7.3) or 2015 (for DA, section 8) were used.

6.2 River masking and processing

The data were delivered in form of point data, and had to be filtered for observations over the water surface of interest. Classification of water returns and land surface returns based directly on the altimetry data itself is difficult. Typically, a water mask is used to filter the relevant data points.

For this PhD study river masks with a resolution of 30 metres were produced. These binary river masks were based on Landsat 7 and Landsat 8 Normalized Difference Vegetation Index (NDVI) derived from optical and NIR imagery. NDVI, or the similar Normalized Difference Water Index (NDWI) have repeatedly been used to delineate water surfaces (Birkinshaw et al., 2014; Michailovsky et al., 2012; Neal et al., 2012; O'Loughlin et al., 2013). For this case, all pixels with a NDVI value of 0 or less were considered water surface. The Brahmaputra River in the downstream Assam valley is a dynamic braided river, experiencing relevant changes to water extent during the flow seasons and to river channel location. Consequently, one individual river mask was constructed for each year. Each mask is a conservative estimate of water extent, i.e. representing low-flow conditions. Cloud cover limits the availability of optical imagery over the Brahmaputra River, and prohibits derivation of river masks at higher temporal resolution. The Po River and the upstream parts of the Brahmaputra River are less dynamic; static masks were used here. The water level observations were projected onto the respective river

lines. The masking process is illustrated in Figure 5, for an example over the Brahmaputra River.

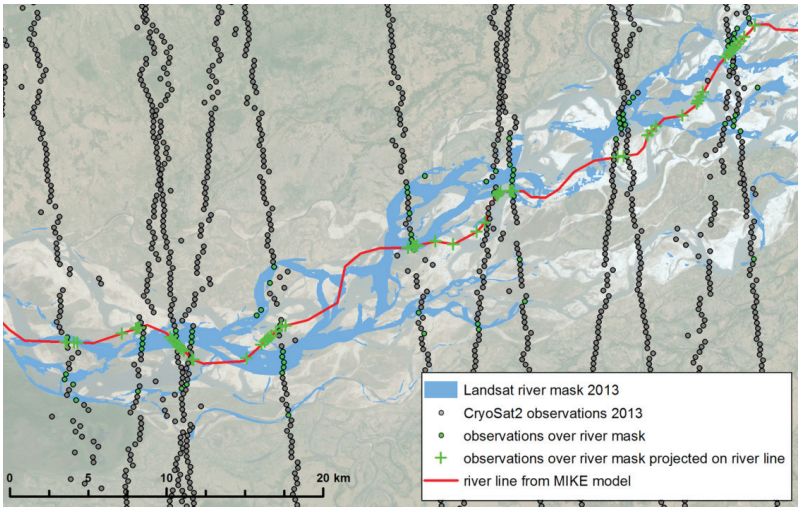

Figure 5. Detail of the Brahmaputra River showing the Landsat river mask and CryoSat-2 observations for the year 2013, including the mapping to the river line. This method was applied for both the Brahmaputra and the Po River. From Paper III.

Lastly, outliers were filtered: A very rough filtering was performed by defining a maximum threshold for the difference between the observed water levels and the respective surface heights of a DEM such as the data from the Shuttle Radar Topography Mission (SRTM), as done in Paper III over the Brahmaputra River. The threshold value was set to 20 metres. Another approach is to define a threshold deviation from a fitted mean water level along the river, as done in Paper II over the Po River. This threshold value was set to 5 metres, in accordance with the maximum amplitude observed at in situ gauging stations.

Figure 6 displays the masked CryoSat-2 water level observations along the two rivers. For the Po River, it can be seen that the CryoSat-2 observations nicely follow the observed water levels at in situ stations, which are displayed with their 90 % quantiles. The step around river km 370 is related to a dam at Isola Serafini. A detailed evaluation of the accuracy of CryoSat-2 follows in section 6.3.

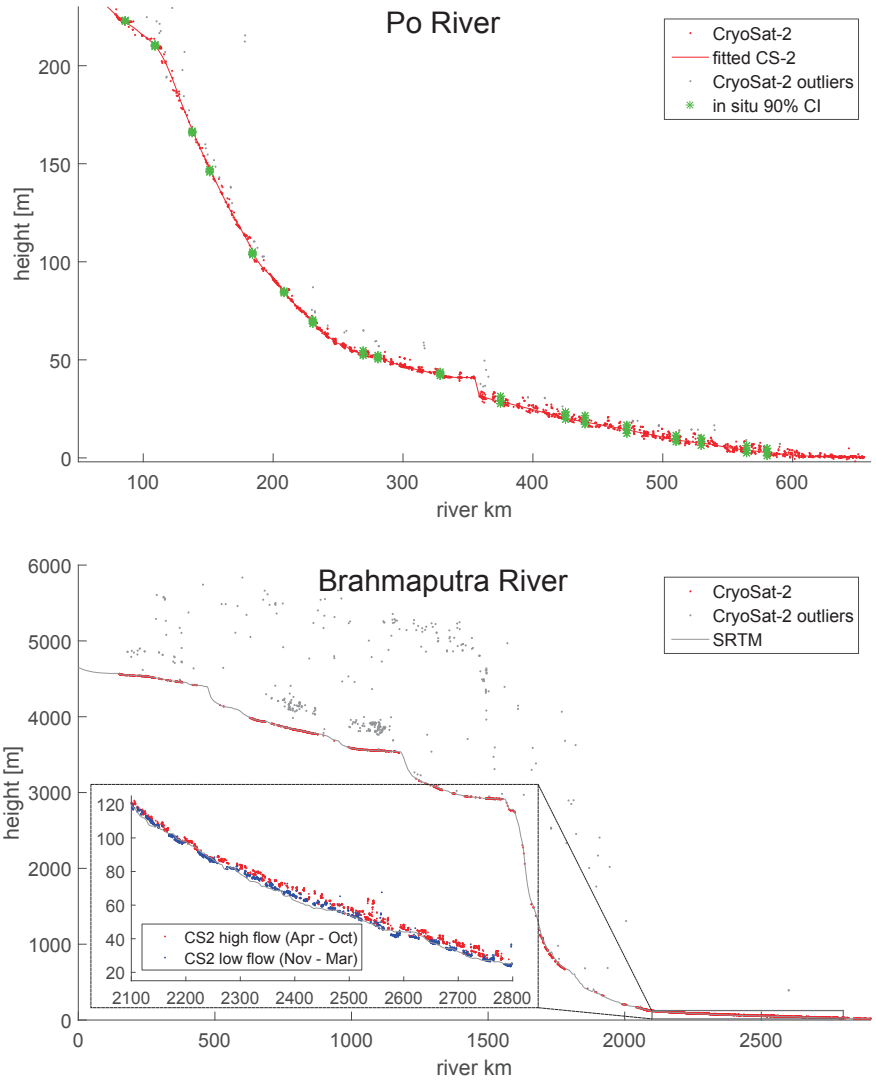

Figure 6. CryoSat-2 data over the Po (top) and Brahmaputra (bottom) rivers. The inlet for the Brahmaputra River shows the downstream Assam valley.

For the Brahmaputra River, two regions have to be distinguished: The upstream region, where the river is relatively narrow and partly flowing through steep valleys, and the downstream region starting at around river km 2100 which is referred to as Assam valley (indicated in Figure 4). In the upstream region, a large number of extreme outliers exist in the CryoSat-2 data. Most

likely, these outliers originate from the open-loop control of the range window on CryoSat-2, which fails to follow rough topography like it is found in the Himalayan mountains (Dehecq et al., 2013). This indicates that a closed-loop control, using a DEM stored on board of the altimeter to adapt the range window, could significantly increase performance over inland waters in challenging topography. Still, more than 80 % of the CryoSat-2 observations remain after the applied outlier filtering (Table 2). For the downstream Assam valley (inlet in Figure 6) almost no outliers exist. The sampling of CryoSat-2 along the river (for example around river km 2200 and km 2700) exhibits some seasonal pattern. Discharge in the Brahmaputra River has a clear seasonal pattern, with a flood peak in summer. Dependent on the orientation of the river, CryoSat-2 with its repeat cycle of 369 days (approximately one year) will sample certain stretches of the river predominantly at certain times of the year. This has to be considered when deriving river water level profiles from the data.

Table 2. Number of CryoSat-2 observations for the two case studies. Brahmaputra river km 2100-2800 refers to the Assam valley which is focus of the cross section calibration and DA. Po river km 225-660 refers to the downstream part, which is focus of the in situ validation of the CryoSat-2 data. Data for the Brahmaputra River from 2010 to February 2015 (extended compared to Paper III), for the Po River from 2010 to 2016.

	observations, total	outliers	observations, outlier filtered	river transects, outlier filtered
Brahmaputra km 0-2100	2371	387* (16.3 %)	1984	624
Brahmaputra km 2100-2800	4453	3 (0.1 %)	4450	705
Po km 0-225	390	42 (10.8 %)	348	149
Po km 225-660	1912	43 (2.2 %)	1869	655

*another 935 observations exist where the retracking failed to deliver a surface height

The width of the river is reflected in the number of individual observations per river transect ("transect" refers to a single crossing of the river by the satellite ground track). For the downstream part of the Po River, there are on average only 2.9 individual observations per transect. For the wider Brahmaputra River in the downstream Assam valley, there are on average 6.2 observations per transect. This allows some along-track evaluation of single transects.

6.3 Validation of CryoSat-2 against in situ data

So far, evaluation of CryoSat-2 altimetry data over rivers has been limited (Paper I). The few available studies (Bercher et al., 2013; Villadsen et al., 2015, 2016) validated CryoSat-2 data against single in situ station data or altimetry data from other missions. The results indicate that CryoSat-2 performs similar or slightly better than previous altimeters, i.e. errors over rivers of 0.5 metres or less can be expected. The Po River was chosen as for the validation, as it (i) is covered by all three operational modes of CryoSat-2 (LRM, SAR, SARIn), (ii) has a dense network of in situ gauging stations, and (iii) is a relatively narrow river, ensuring transferability of the results to many other rivers.

Hourly water level observations from 18 gauging stations along the Po River (Figure 4) are available from the Interregional Agency for the Po River (AIPo). To allow direct comparison of absolute water levels, all elevations were converted to a common height reference, the local Italian geoid ITALGEO 2005 (Barzaghi et al., 2007). A systematic bias in water level observations from altimetry missions commonly exists. This bias was estimated by comparing the CryoSat-2 observations over sea against a tide gauge, indicated in Figure 4. Finally, the CryoSat-2 observations along the river were compared to the closest in situ station. The elevation values of the CryoSat-2 observations were transferred by correcting for estimated river slope. For details please refer to Paper II.

Table 3 presents the results of the in situ validation, for all CryoSat-2 observations within 3 km of in situ stations. The 3 km-window was found to offer a good trade-off between the number of observations evaluated and additional error introduced from the slope correction: For the 12 downstream stations, increasing the window size to 5 km allows the evaluation of 478 observations with a RMSE of 0.44 m, and a window size of 10 km evaluates 916 observations with a RMSE of 0.60 m, compared to 266 observations with a RMSE of 0.38 m for the 3 km window. The performance along the six upstream stations (grey in Figure 4 and Table 3) is considerably worse than for the twelve downstream stations. Reasons for this are the river width, decreasing from 250 to 350 m along the downstream stations to 75 m for the upstream stations. Also, the upstream part of the Po River is steeper, which leads to higher errors from the slope correction.

Table 3. Results of validation of CryoSat-2 data against in situ stations, within 3 km of each station. The 6 upstream stations are greyed out due to bad performance. Data from 2010 to 2016. Detailed results can be found in Paper II.

	12 downstream stations				6 upstream stations			
	all	LRM	SAR	SARIn	**all**	LRM	SAR	SARIn
no. of obs.	**266**	91	135	40	**78**	37	12	29
RMSE [m]	**0.38**	0.34	0.40	0.37	**1.36**	1.46	0.90	1.32
ME [m]	**-0.16**	-0.06	-0.20	-0.25	**-0.57**	-0.56	-0.30	-0.65

The results, with an average RMSE of 0.38 m along the downstream stations, are encouraging. Probably a better bias estimate could further improve the results as a consistently negative ME is observed. Still, CryoSat-2 observations errors are within ranges reported in literature for other missions, often evaluated over rivers wider than the Po River, and calculated not for absolute water levels, but for water level anomalies: Over rivers such as the Amazon, Mekong, or Zambezi, validation studies found errors between approximately 10 cm and 1 m compared to in situ data (Villadsen et al., 2016). Over the more narrow Garonne River, Biancamaria et al. (2017) found a RMSE between approximately 0.2 m and 0.7 m for river widths of around 200 m. For CryoSat-2 over the Po River, all three modes seem to be performing equally well. This indicates that for application over rivers, the advanced altimeter modes SAR and SARIn are not superior, and allows global use of CryoSat-2 data.

7 Use of CryoSat-2 to parameterize hydrodynamic river models

The potential of CryoSat-2 altimetry data to parameterize hydrodynamic river models was evaluated using a 1D hydrodynamic river model for each case study. The high spatial resolution of CryoSat-2 altimetry data proved to be particularly useful. Two fundamentally different cases are considered: The Po River as a gauged river, where detailed data of cross section geometry and the like are available, and the Brahmaputra River as an ungauged or poorly gauged basin, where none of these data are available. For the gauged Po River, channel roughness was calibrated (section 7.2), allowing a finer spatial resolution than possible with in situ data. For the ungauged Brahmaputra River, cross section shapes were calibrated (section 7.3), so that the model accurately reproduces water level-discharge relationships. An overview of the two calibrations detailed in the following is given in Figure 7 and Table 4.

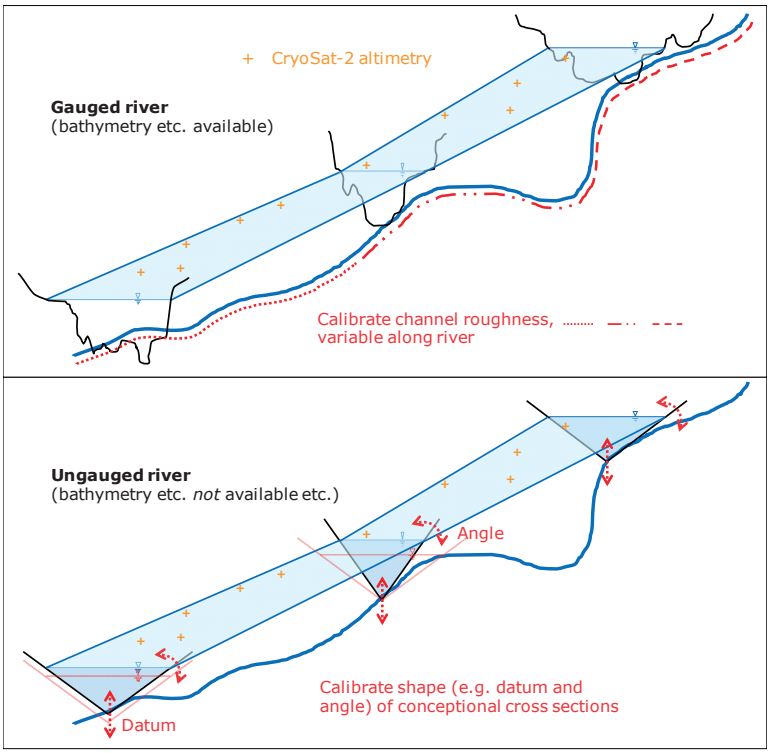

Figure 7. Calibration of hydrodynamic river models using CryoSat-2 data, for gauged (top) and ungauged (bottom) rivers.

Table 4. Overview of the two cases for hydrodynamic model calibration using CryoSat-2 data.

	Gauged river	**Ungauged river**
Model setup	Dense network of surveyed cross sections	Conceptual cross sections (triangular) at defined interval
Calibration parameters	Channel roughness, with different spatial resolution	Cross section shapes (i.e. angles) and datums along river network
Calibration objective	minimize RMSE between simulated water levels and CryoSat-2 observations	
Calibration constraints	optional: smoothness constraint, upper and lower limits	optional: smoothness constraint, continuously decreasing cross section datums, upper and lower limits
Used optimization algorithm	Non-linear least squares solver (MATLAB lsqnonlin)	Non-linear least squares solver or genetic algorithm (MATLAB lsqnonlin or ga)

7.1 MIKE HYDRO River hydrodynamic model

There exist numerous possibilities to model river flow: from simple routing schemes such as the Muskingum or Muskingum-Cunge schemes, to various 1D or 2D hydrodynamic models. Also, different versions of coupled 1D-2D models exist. Simple, but computationally less expensive models omit, for example, backwater effects, which are important for low-gradient rivers such as the Brahmaputra. On the other hand, the most advanced 2D or 1D-2D models are computationally expensive, which usually limits their large-scale applications to deterministic simulations (Biancamaria et al., 2009, 2011a; Schumann et al., 2013).

For the two case studies, a DHI MIKE HYDRO River (DHI, 2015, previously referred to as MIKE 11) 1D hydrodynamic model was set up. This was considered a reasonable trade-off between computational efficiency and realistic flow routing. Such a 1D hydrodynamic model offers the possibility to perform a large number of model runs, which is relevant for calibrating the model (section 7) and for DA applications based on ensemble filters (section 8) or other probabilistic analysis. The hydrodynamic model in MIKE HYDRO River uses a 1D dynamic wave routing based on the Saint-Venant equations for unsteady flow (Havnø et al., 1995). Its governing equations are solved by a 6-point implicit finite difference scheme (Abbott and Ionescu, 1967) on a staggered grid of alternating Q and h points as displayed in Figure 8: discharge is calculated at Q points, water level is calculated at h points. h points are placed at cross sections and, at large cross section distances, also in between.

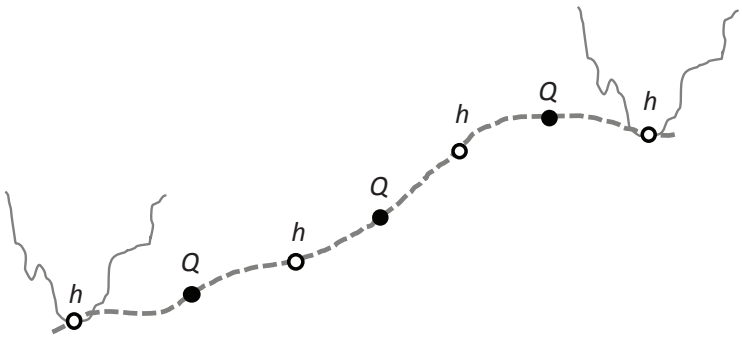

Figure 8. Sketch of the computational grid of MIHE HYDRO River. Defined cross sections at the first and last h point. Interpolated cross sections at h points in between not displayed.

For the Po River the focus was on the river routing. The hydrodynamic model of the downstream part of the Po River was set up using surveyed cross sections. The model was forced by observed discharge at the upstream boundary Cremona and by observed discharge from the tributaries. Simulation results can be evaluated at eight in situ stations along the river (all indicated in Figure 9).

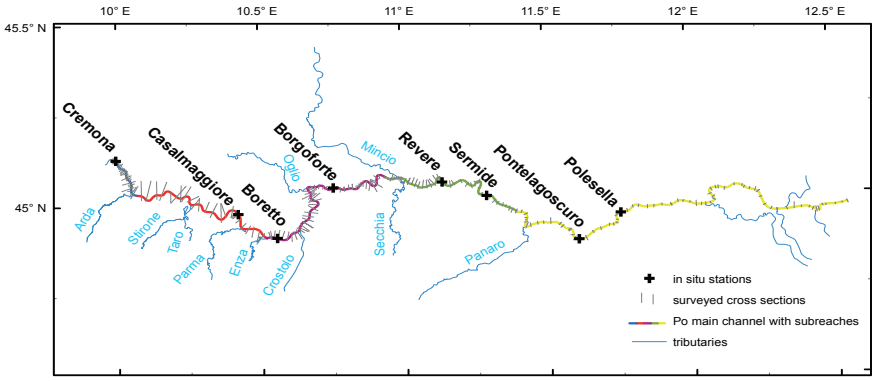

Figure 9. Sketch of the MIKE HYDRO River hydrodynamic river model of the Po River, including the tributaries that are part of the discharge forcing. The partitioning into five subreaches for the roughness calibration is colour coded. From Paper II.

For the mostly ungauged Brahmaputra River, however, a hydrologic-hydrodynamic basin model was set up (Figure 10). This model encompasses the entire basin down to Bahadurabad station close to the confluence of the Brahmaputra with the Ganges River and is almost exclusively based on remote sensing data. The hydrologic part consists of 33 subcatchments; each of them modelled as a lumped, conceptual NAM rainfall-runoff model (Nielsen and Hansen, 1973). Precipitation, temperature and evaporation forcing is derived from the TRMM v7 3B42 (Tropical Rainfall Measurement Mission Project (TRMM), 2011) and ERA-Interim products (Berrisford et al., 2011; Dee et al., 2011). Calibration of the rainfall-runoff models had to be performed based on a very limited number of stations observing subcatchment discharge, and was done in conjunction with a model of the neighbouring Ganges Basin. More details can be found in Paper III. The simulated runoff then forces the hydrodynamic model of the river network. Delineation of the

subcatchments and river network was based on the SRTM DEM. Evaluation of the total basin outflow was performed at Bahadurabad station where in situ water level and discharge are available.

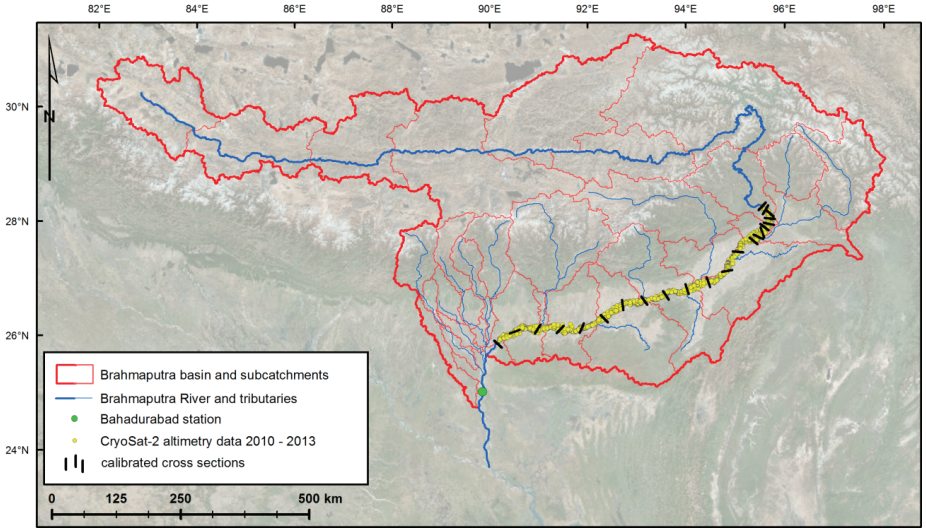

Figure 10. Overview of the MIKE HYDRO River hydrologic-hydrodynamic model of the Brahmaputra Basin, including the CryoSat-2 data used in the cross section calibration.

7.2 Channel roughness calibration in gauged rivers

For a hydrodynamic river model with surveyed cross sections which is forced by observed discharge, the remaining uncertainty (disregarding conceptual model uncertainty) is essentially due to the channel roughness. River channel roughness cannot be observed directly. Even though remote sensing data are used to aid estimation of channel roughness (Bates et al., 2014), it is commonly treated as a calibration parameter (Morvan et al., 2008). The matter is complicated by the fact that model channel roughness not only accounts for the roughness of the surface as such, but incorporates other river characteristics such as channel curvature (Chow, 1959; James, 1994). This is especially valid for 1D or coupled 1D-2D river models that do not incorporate river bends in the model structure. River channel roughness varies along the river and across the river cross section (floodplains usually have higher roughness than the constantly submerged parts of the channel, etc.). The ability to re-

solve this variability in calibration, however, is limited by the spatial distribution of observation data used in the calibration (for example Hostache et al., 2010; Pappenberger et al., 2005). Conventionally, roughness is calibrated to a homogenous value along the entire river or in relatively long subreaches. This applies to the Po River, too, where water level data are available from a relatively dense network of in situ stations with a spacing of 15 to 50 km.

Two subdivisions of the Po River were investigated in this study. The first, conventional subdivision in five subreaches is shown in Figure 9. It was suggested for the Po River similarly by Zannoni, 2010 and adopted before for hydraulic model calibration (Castellarin et al., 2011; Domeneghetti et al., 2014). The channel roughness for the five subreaches was calibrated to minimize the RMSE between observed and simulated water levels

$$OV = \sqrt{\frac{1}{n}\sum_{i=1}^{n}(h_{obs,i} - h_{sim,i})^2} \quad (1)$$

CryoSat-2 data are distributed continuously along the river, which makes it possible to parameterize channel roughness variably along the river model (Figure 7 top): channel roughness was defined in 10 km long sections. This second investigated subdivision gave a total of 29 sections with individual roughness instead of the five subreaches. To avoid model overfit with such a large number of parameters, a smoothness constraint was included in the objective value *OV* for the calibration alongside with RMSE between observed and simulated water levels

$$OV = \sqrt{\frac{1}{n+m}\left(\sum_{i=1}^{n}(h_{obs,i} - h_{sim,i})^2 + f\sum_{i=1}^{m}(r_{i+1} - r_i)^2\right)} \quad (2)$$

where there exist n observations and m roughness sections, and h_{obs} and h_{sim} refer to observed and simulated water levels, respectively. r are the roughness values as Manning's M [$m^{1/3}\ s^{-1}$]. The entire second term, which has to be weighted by a factor f, considers the differences between neighbouring roughness values. I.e. highly variable roughness patterns will be penalized in the calibration.

Both river subdivisions were calibrated against (i) in situ water level data only, (ii) CryoSat-2 data only, and (iii) a combination of in situ and CryoSat-2 data. Details can be found in Paper II. The main results are summarized in Table 5: CryoSat-2 data proved to be well suited to calibrate the channel roughness in the conventional setup with five subreaches. Calibration against CryoSat-2 data (row 3) instead of in situ data (row 1) lead only to a minor

deterioration of the performance against in situ data. In general, introducing variable channel roughness lead to a better model fit. Table 5 also presents the average width of the confidence intervals (CI) of the fitted Manning's *M* parameters. The CI can be derived from the solution of the non-linear least squares solver and indicate how well the data can define the model parameters. Using in situ data only in the calibration can hardly define the roughness in 10 km sections. CryoSat-2 data, however, can better define the variable roughness.

Table 5. Results of the channel roughness calibration of the Po River model together with their calibrated parameter confidence intervals (CI). High and medium smoothness weight refer to different factors *f* in equation (2). S1 to S3 refer to Figure 11.

setup	calibrated against	RMSE in situ [m]	RMSE CS-2 [m]	avg. width of Manning's *M* 95 % CI [$m^{1/3}$ s^{-1}]
5 subreaches	in situ **S1**	0.289	0.643	0.2
	in situ and CS-2	0.291	0.639	0.5
	CS-2	0.310	0.634	4.1
10 km sections, medium smoothness weight	in situ	0.260	0.610	37.8
	in situ and CS-2	0.262	0.573	1.5
	CS-2 **S2**	0.311	0.563	13.8
10 km sections, high smoothness weight	in situ	0.269	0.616	21.1
	in situ and CS-2	0.267	0.595	0.8
	CS-2 **S3**	0.282	0.583	7.4

Figure 11 presents the calibrated Manning's *M* values along the river for three calibration setups: S1 refers to the model with five subreaches, calibrated against in situ data. S2 and S3 both have variable channel roughness and are calibrated against CryoSat-2 data, but differ in the weighting factor *f* applied to the smoothness constraint in equation (2). A higher weight on the smoothness constraint leads to less variable channel roughness, but better defined parameters. The distribution of the variable channel roughness from S2 and S3 roughly follows the values obtained with the five subreaches model S1. As discussed in the beginning of the section, the channel roughness also accounts for river curvature etc. River curvature can be expressed as sinuosity, where the minimum value of 1 stands for a straight river, and higher values for a more and more curved river (for details please refer to Paper II). It could be shown that there is a slight correlation between river sinuosity and

the variable channel roughness with a coefficient of correlation R^2 of up to 0.25.

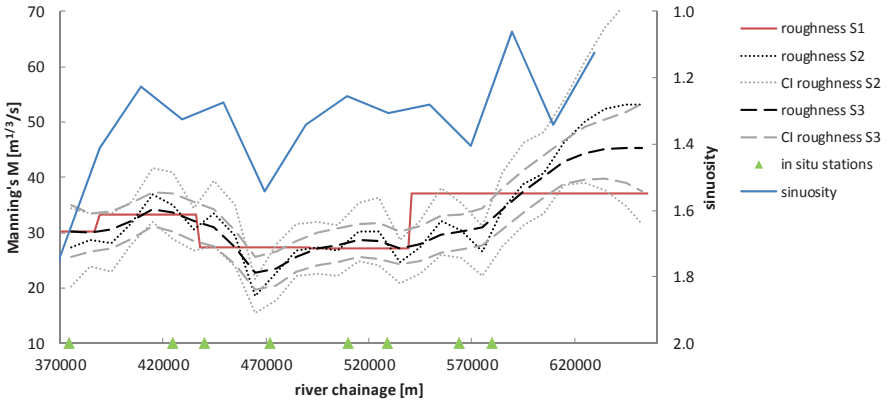

Figure 11. Roughness from calibrations setups S1 to S3 (compare Table 5). The calibrated variable roughness values are displayed together with their 95 % CI. River sinuosity on the right y-axis. Location of in situ stations indicated on x-axis. Adapted from Paper II.

Despite (i) the availability of surveyed cross sections and other in situ data, (ii) the lower temporal resolution of CryoSat-2 observations, and (iii) their higher observation error compared to in situ observations, CryoSat-2 still provides additional information for the parameterization of the Po River model. This is thanks to the unique spatio-temporal distribution of CryoSat-2 data which means that observations exist basically all along the river, instead of at in situ stations or virtual stations from conventional satellite altimetry. In a very similar case study, Domeneghetti et al. (2014) calibrated channel roughness in a model of the Po River using virtual station data from ERS-2 and Envisat. They concluded that "satellite data do not seem yet capable of completely substituting in-situ observations". The work presented here can be seen as moving a step closer to overcoming this.

7.3 Cross section calibration in poorly gauged rivers

For a poorly gauged river precise river bathymetry information is not available. Cross section shapes for large-scale hydrodynamic models can, for example, be derived from globally available DEMs such as SRTM, which probably still is the most commonly used (Domeneghetti, 2016; Md Ali et al.,

2015; Pramanik et al., 2010; Yan et al., 2013). However, those DEMs do not provide information about the submerged part of the river cross section, which leads to various estimation methods applied in the above mentioned studies. Relative and absolute surface height errors of SRTM data are considerable with up to 10 m. Also, SRTM data include vegetation heights. Yan et al. (2015) review the challenges of using global DEMs in the context of flood modelling.

This study suggests an alternative to parameterizing cross sections shapes in rivers lacking bathymetry information: The distributed water level observations from CryoSat-2 were used to calibrate shape and datum of synthetic cross sections. Triangular cross sections were placed at regular intervals (indicated in Figure 10). Two parameters for each cross section, the datum and the opening angle of the triangular shape (Figure 7), were calibrated by fitting the simulated water levels to CryoSat-2 water level observations. Initially, as reported in Paper III, the calibration of cross section angles and cross section datums was separated into a two-step iterative process. This included the use of Envisat virtual station water level observations for the calibration of the cross section angles. CryoSat-2 data were only used to calibrate the cross section datums. Later, however, it could be shown that CryoSat-2 data alone are sufficient to calibrate both cross section datums and angles simultaneously: the simulated water levels were fitted to the CryoSat-2 observations using a non-linear least squares solver, instead of the genetic algorithm used in Paper III. Figure 12 displays the results. An average RMSE between CryoSat-2 observed water levels and simulated water levels of 1.24 m was achieved with the calibrated model. The remaining error is considerable, however, a part of this error must be attributed to the errors in the runoff forcing of the model, and not to the cross section parameterization. The actual water level-discharge relationship may be modelled with higher accuracy. Even though the representation of the river geometry is not realistic, it is assumed that the derived cross section shapes have some physical meaning. For example the narrowing of the river around river km 2600 in the calibrated cross sections can also be observed in reality, as shown in Figure 13.

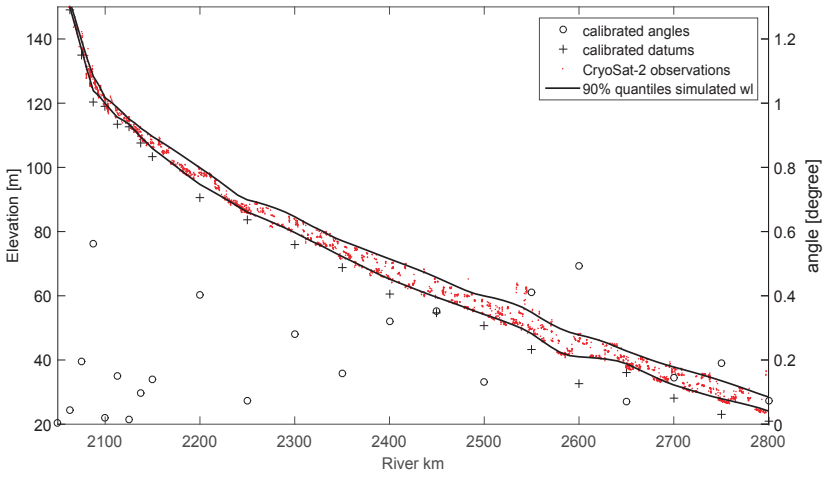

Figure 12. Results of the synthetic cross section calibration along the Assam valley. The 90 % quantiles of the best fit simulated water levels are displayed together with the CryoSat-2 observations and the calibrated cross section datums and angles.

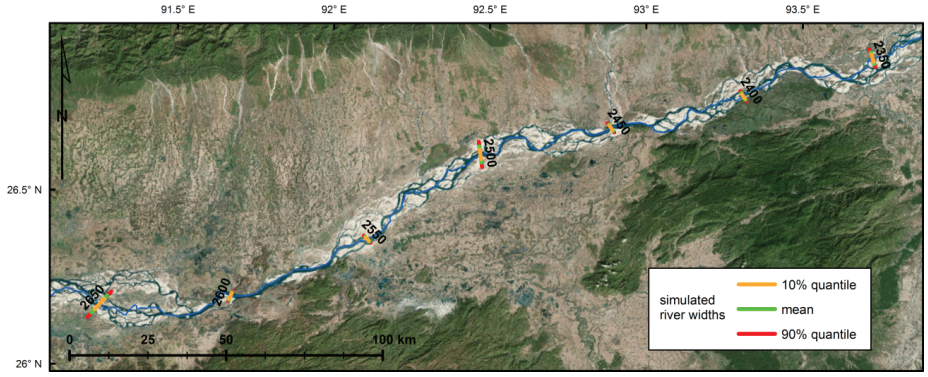

Figure 13. Simulated river widths after calibration of the triangular cross sections, for the 10 % and 90 % water level quantiles and the mean. River km labelled on the cross sections.

It is assumed that after the calibration the model accurately represents absolute water level dynamics along the entire river. Generally, this cannot be achieved easily in ungauged basins. It is, however, prerequisite to compare simulated water levels to distributed observations of water level, such as from CryoSat-2. To avoid having to work with absolute water levels, some prior studies integrating satellite altimetry data with models of ungauged rivers

have relied on using water level amplitudes or applied bias correction at each virtual station (Hossain et al., 2014; Michailovsky et al., 2013; Paiva et al., 2013). This is not possible with CryoSat-2 data. Hence, the cross section calibration is a preparatory task for the DA experiments that are outlined in the following sections.

8 Use of CryoSat-2 data to update hydrodynamic river models

8.1 Data Assimilation

Data assimilation (DA) refers to the merging of model simulations with information from model-independent observations. Examples of applications of DA in hydrology have been briefly discussed in section 4.6. In this case, DA was used to update water levels in a hydrodynamic river model using satellite altimetry observations from, for example, CryoSat-2. Generically, such a model can be expressed as

$$\mathbf{x}_t = \mathbf{M}_t(\mathbf{x}_{t-1}) + \mathbf{w}_t \tag{3}$$

where $\mathbf{x}_t$ is the state vector constituting the state of the modelled system. It is propagated from time $t-1$ to t by the model operator (or simply: the model) $\mathbf{M}_t$. The model operator includes parameter values, forcing, and similar data defining the model setup. All model errors are summarized in the term $\mathbf{w}_t$. The state vector is related to the observations $\mathbf{y}_t$ via the observation operator $\mathbf{H}_t$

$$\mathbf{y}_t = \mathbf{H}_t\mathbf{x}_t + \mathbf{v}_t \tag{4}$$

where $\mathbf{v}_t$ represents the observation uncertainty. Usually, DA is applied to update models sequentially. Each time an observation becomes available, the model is updated considering the observation. This step is called analysis:

$$\mathbf{x}_t^a = \mathbf{x}_t^f + \mathbf{K}_t(\mathbf{y}_t - \mathbf{H}_t(\mathbf{x}_t^f)) \tag{5}$$

$\mathbf{x}_t^f$ is the model forecast, i.e. the state vector propagated from previous time steps by the model. $\mathbf{x}_t^a$ is the updated state vector, resulting from the analysis. In the same step, the covariance matrix between the forecasted model states $\mathbf{P}_t^f$ is updated

$$\mathbf{P}_t^a = \mathbf{P}_t^f - \mathbf{K}_t\mathbf{H}_t\mathbf{P}_t^f \tag{6}$$

The gain operator $\mathbf{K}_t$ weights between model forecast and observation dependent on the related uncertainties and correlations between state variables, and is defined as

$$\mathbf{K}_t = \mathbf{P}_t^f\mathbf{H}_t^T[\mathbf{H}_t\mathbf{P}_t^f\mathbf{H}_t^T + \mathbf{R}_t]^{-1} \tag{7}$$

where $\mathbf{R}_t$ is the covariance matrix of the observation errors. Given that both model and observation uncertainty are described adequately, the combination of these two sources of information in the DA analysis reduces the prediction uncertainty of the model.

Often, DA algorithms are based on the Kalman Filter (KF) (Jazwinski, 1970; Maybeck, 1979). The original implementations of the KF require explicit formulations of the covariance matrix of the model state and its propagation through time. This limits its use to linear models of relatively low order. The extended KF allows to slightly extend the applicability, as for example done by Michailovsky et al. (2013) for a Muskingum routing scheme. Many hydrologic models are too complex to allow explicit formulations of equations (5) to (7) etc. (Reichle et al., 2002). They, however, can be updated using ensemble based methods such as the Ensemble Kalman Filter (EnKF) (Evensen, 1994, 2003). EnKF and related methods are popular for a wide range of hydrologic applications (Liu et al., 2012). Ensemble based KF represent the state space by an ensemble of models. From this ensemble, the model state covariance matrix $\mathbf{P}$ is estimated via

$$\mathbf{P} = \frac{1}{m-1}\sum_{i=1}^{m}(\mathbf{X}_i - \mathbf{x})(\mathbf{X}_i - \mathbf{x})^T = \frac{1}{m-1}\mathbf{A}\mathbf{A}^T \tag{8}$$

where $\mathbf{X} = [\mathbf{X}_1, ..., \mathbf{X}_m]$ represents the ensemble of model state vectors, with size m and the ensemble mean $\mathbf{x} = \frac{1}{m}\sum_{i=1}^{m}\mathbf{X}_i$. $\mathbf{A} = [\mathbf{A}_1, ..., \mathbf{A}_m]$ are the ensemble anomalies.

For this study, the Ensemble Transform Kalman Filter (ETKF) was used. It was originally suggested by Bishop et al. (2001) and used in an implementation based on Sakov and Oke (2008). One advantage of the ETKF over the EnKF is that it does not require perturbation of the assimilated observations as it updates the ensemble anomalies explicitly

$$\mathbf{A}^a = \mathbf{A}^f\mathbf{T} \tag{9}$$

with

$$\begin{aligned} \mathbf{T} &= \mathbf{T}^S\mathbf{U} \\ \mathbf{T}^S &= \left[\mathbf{I} + \frac{1}{m-1}(\mathbf{H}\mathbf{A}^f)^T\mathbf{R}^{-1}\mathbf{H}\mathbf{A}^f\right]^{-1/2} \end{aligned} \tag{10}$$

where $\mathbf{T}$ is referred to as the ensemble transform matrix and $\mathbf{U}$ is an arbitrary orthonormal matrix. This theoretically leads to better filter results. For details of the ETKF please refer to Sakov and Oke (2008) and Hunt et al. (2007).

8.2 DHI MIKE HYDRO River Data Assimilation framework

For the DA experiments the DHI Data Assimilation Framework was used. It is coded in .NET/C#. The DA framework initially had been developed in conjunction with the catchment modelling toolkit MIKE SHE (Ridler et al., 2014), and then adapted to work with the river modelling software MIKE HYDRO River. During this PhD study, it has been debugged, modified and tested, mainly based on the Brahmaputra River model. Figure 14 provides a conceptual overview.

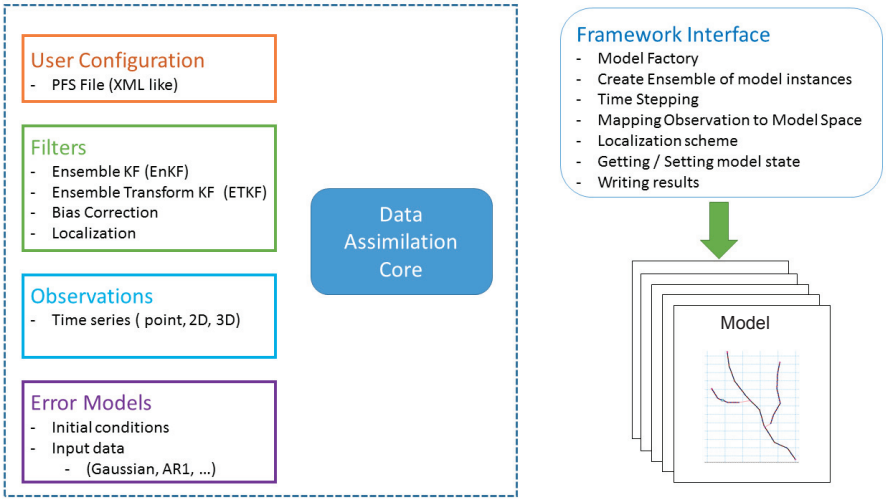

Figure 14. Sketch of the DHI MIKE HYDRO River data assimilation framework. From Paper IV.

The main advantages of the used DA framework are that it is fully coupled with MIKE HYDRO River via a framework interface, allowing computationally efficient updates of the model. Furthermore, it integrates all DA related tasks, such as the creation of the model ensemble, the observation mapping, or the state updating. It provides a number of generic assimilation filters, procedures for localization, methods to describe model and observation noise, observation mapping, etc. The different options are defined in an ASCII format configuration file. A more detailed description of the general capabilities of the DA framework can be found in Paper IV. The specific DA setup used

in this study in combination with the Brahmaputra River case study is described in the following section.

8.3 DA case study: Brahmaputra River

First, one has to decide which part of the state vector is to be updated. In principle, all *h* and *Q* points in the model (see Figure 8) should be updated. However, with the given numerical scheme, an update of *h* implicitly also leads to an update of *Q* (Madsen and Skotner, 2005). In synthetic experiments it could be shown that there is no significant difference between updating *h* only or *h* and *Q*. Therefore, the state vector was populated only by the water heights in the *h* points.

Another crucial aspect of DA is the appropriate representation of model uncertainty. In ensemble based KF methods, the model uncertainty is represented by the model ensemble which commonly is created by perturbing relevant forcings or parameters. For large-scale hydrodynamic models of poorly gauged rivers as in this case, the main source of model error is considered to originate from simulated runoff, which is largely driven by climate forcing. The most sensitive forcing of hydrologic models is precipitation (Sorooshian et al., 2009). Hence, for DA applications either the climate forcing of the hydrologic models (Biancamaria et al., 2011a; Paiva et al., 2013), or the runoff generated by those models (Andreadis et al., 2007; Michailovsky et al., 2013) can be perturbed to obtain a representation of model error. For the Brahmaputra River case, the runoff generated in the subcatchments was perturbed. The perturbations are expected to be correlated temporally and spatially. This was achieved by applying an additive, spatially correlated first-order autoregressive (AR(1)) perturbation error:

$$\begin{aligned} \mathbf{f}_p &= \mathbf{f}_u(1+\mathbf{e}_t) \\ \mathbf{e}_t &= (\delta \mathbf{e}_{t-1} + \boldsymbol{\varepsilon}_t)\mathbf{L} \\ \boldsymbol{\varepsilon}_t &\sim \mathcal{N}(0, \sqrt{(1-\delta^2)a^2}) \end{aligned} \tag{11}$$

where $\mathbf{f}_p$ and $\mathbf{f}_u$ are the vectors of the perturbed and unperturbed runoff forcings from all subcatchments, respectively. $\mathbf{e}_t$ is the vector of additive perturbations, δ the AR(1) parameter, and $\boldsymbol{\varepsilon}_t$ a vector of white Gaussian noise. a is a factor to scale the Gaussian noise. $\mathbf{L}$ is the Cholesky decomposition (Kay, 1988, chap. 6) of the correlation matrix $\mathbf{C}$ of the subcatchment forcings. Specific values for a and δ were estimated based on evaluation of the in situ discharge residuals at Bahadurabad station.

Due to limited ensemble size, models are prone to exhibit spurious correlations in the derived model state covariance matrix **P** (equation (8)). This leads to erroneous updates. To avoid such issues, the update can be limited to affect only parts of the model, usually closest to the current observation. This is referred to as localization (Evensen, 2009, chap. 15) and was implemented for the ETKF as described by Sakov and Bertino (2011).

The time step of hydrodynamic models is small compared to the dynamics of river flow. In this case the numerical scheme was solved at 5-minute intervals. It is reasonable to assume that a water level observation delivers information about a longer time frame than a single simulation time step. This was accounted for by applying the updates over the time frame of a so-called virtual window.

For further details of the applied DA approach the reader is referred to Paper IV. Table 6 provides an overview of the specific parameters used for the Brahmaputra River case.

Table 6. Overview of Brahmaputra River model DA parameters. Symbols refer to equation (11). Details are reported in the supplementary material of Paper IV.

Parameter	Value	Remarks
Amplitude of relative perturbation error a	0.3	Derived from ensemble coverage of discharge at Bahadurabad station in open loop experiments.
AR(1) factor of relative perturbation error δ	0.96	Equal to temporal correlation of relative discharge error at Bahadurabad station.
Spatial correlation $\mathbf{C}$	0.76 (mean)	Equal to spatial correlation of simulated subcatchment runoffs.
Localization size	200 km around observation	Largest value possible without experiencing unreasonable updates causing the model to crash. Entire river model is ~1200 km long.
Virtual window	120 minutes	Derived from simulated water level dynamics, to keep errors from assumption of constant observed water levels negligible. Simulation time step is 5 minutes.
Ensemble size	80	Value chosen based on evaluation of performance of synthetic DA experiments with changing ensemble size, and considering its trade-off with computational effort.

Due to the river width, each transect of the river by CryoSat-2 delivers several individual observations (Figure 5). These observations occur at the exact same point in time and, consequently, represent the same water level. They

were not used individually, but grouped and averaged to update the model. In case of a (near-) perpendicular transect of the river this grouping is straightforward. In cases where the ground tracks of CryoSat-2 and the river are more aligned, however, the observations from a single transect can extend over a considerable distance along the river (e.g. in the north eastern corner of Figure 5). Where the observations extend over more than a threshold distance (3 km in the case of the DA experiments), the observations were grouped into a number of clusters based on their location along the river line using k-means clustering. Assuming that individual observations of each group should have recorded the same water height, their spread can be used as an estimate of observation uncertainty. The averaged observations then were assimilated to the model. Furthermore, additional outlier filtering was applied at this step: The CryoSat-2 observations were compared to the simulated water levels, and considered outliers if they were deviating by more than a certain threshold value. Outlier filtering can be necessary because the numerical scheme of the hydrodynamic model is sensitive to abrupt, extreme water level changes. Assimilating observations differing greatly from the simulated water levels can cause model instabilities. In total, 4467 individual CryoSat-2 observations were used in the DA experiments (excluding 86 outliers deviating more than 3 metres from simulated water levels). These 4467 observations were clustered into 973 groups. Details can be found in Paper IV, and are discussed briefly in section 8.5.

All DA experiments reported in the following two sections were evaluated in terms of discharge at the outlet of the Brahmaputra River model, Bahadurabad station. This is the only station along the Brahmaputra River for which in situ observations are available. The model period is from 2010 to February 2015. The ensemble predictions were evaluated in terms of coverage and sharpness. Coverage describes the share of observations that fall into the range of the predictions (in this case defined by their 90 % CI, i.e. expected coverage is 0.9), and the sharpness is the width of this range. Furthermore, the continuous ranked probability score (CRPS) (Gneiting et al., 2005), a popular verification tool for probabilistic forecasts, was used. The CRPS combines coverage and sharpness in one indicator; its optimal value is zero. Also the Nash-Sutcliffe model efficiency coefficient (NSE) was used. It refers to deterministic forecasts and was calculated for the ensemble mean. The optimal value is 1. Open loop model performance serves as a benchmark. An open loop run is a run of the same model ensemble with the same description

of model uncertainty as used in the DA experiments, but without assimilating any data.

8.4 Data Assimilation experiments with synthetic data

Initially, synthetic DA experiments were conducted with the Brahmaputra model. This was done in hidden truth experiments: First, the forcing of the hydrodynamic model was randomly perturbed (as in equation (11)). From the simulated water levels of the perturbed hidden truth run, synthetic water level observations were extracted. Noise was added to account for observation uncertainty. Finally, the synthetic observations were assimilated to the original non-perturbed model. Then, the performance of the DA can be evaluated in comparison to the hidden truth run. Such controlled experiments allow for evaluation of the performance of DA and general capability of the DA framework in absence of any uncertainties or model flaws, as all uncertainties are controlled. Also, it allows testing the influence of different sampling patterns, observation uncertainties, or DA parameters, such as for example the optimal ensemble size.

The following synthetic observations were considered:

- Synthetic observations with spatio-temporal sampling pattern identical to the original CryoSat-2 observations over the Brahmaputra River; with different observation uncertainties.
- Synthetic observations with the CryoSat-2 sampling pattern, however assuming reversed flow direction of the Brahmaputra River.
- Synthetic observations with sampling pattern of the Sentinel-3A and Sentinel-3B missions

Corresponding to the real DA experiments, results were evaluated at Bahadurabad station. Results for two different hidden truth runs (HT 1 and HT 2) are summarized in Table 7. The two hidden truth runs deviate from the original model by different amount, as can be seen in their open loop performances: The open loop run has a higher CRPS compared to HT 1 than HT 2, which means that HT 1 deviates more from the original model than HT 2. An open loop run in comparison with HT 2 is displayed in Figure 15.

Table 7. Results from synthetic DA experiments, in terms of discharge at Bahadurabad station. Average of 4 runs in each row. Error refers to the standard deviation of the zero mean Gaussian observation error. The last column provides the CRPS improvement of the DA run compared to the respective open loop run.

		NSE [-]	sharp-ness [$m^3 s^{-1}$]	cover-age [-]	CRPS [$m^3 s^{-1}$]	CRPS change [%]
HT 1	open loop	0.753	15611	0.773	3793	-
	DA, error 0.2 m	0.885	9439	0.651	2565	32
	DA, error 0.4 m	0.869	9688	0.673	2722	28
	DA, error 0.2 m, west-east flow	0.913	8153	0.782	1996	47
	DA, error 0.4 m, west-east flow	0.909	8728	0.781	2082	45
HT 2	open loop*	0.848	15611	0.839	3305	-
	DA, error 0.05 m	0.912	9672	0.858	2190	34
	DA, error 0.1 m	0.907	9574	0.844	2279	31
	DA, error 0.2 m*	0.909	9256	0.821	2265	31
	DA, error 0.4 m	0.896	9733	0.811	2445	26
	DA, error 1.0 m	0.901	9259	0.693	2544	23
	DA, error 0.2 m, west-east flow	0.911	8267	0.812	2137	35
	DA, error 0.4 m, west-east flow	0.911	8683	0.808	2192	34
	DA, Sentinel-3A, error 0.4 m	0.882	7888	0.746	2388	28
	DA, Sentinel-3A and B, error 0.4 m	0.899	6693	0.661	2182	34

* example runs shown in Figure 15 and Figure 16

An observation error of 0.2 or 0.4 m is considered realistic for current satellite altimetry observations. A run assimilating synthetic observations with an error of 0.2 m is displayed in Figure 16. Assimilation of synthetic CryoSat-2 observations with such observation errors improves the model predictions at the outlet in terms of CRPS by 32 % or 28 % for HT 1, and 31 % or 26 % for HT 2. The observation uncertainties then were further varied for HT 2. Apparently, the value of assimilating CryoSat-2 altimetry data cannot be increased beyond a certain level by reducing the (theoretic) observation error: For HT 2, no large improvement in DA performance can be seen when reducing observation uncertainty from 0.2 m to 0.1 m and 0.05 m. On the other hand, assimilating observations with an error as high as 1.0 m still improves the model. The observation error, of course, has to be seen in relation to the river water level amplitudes, which are large along the Brahmaputra River with up to 10 m.

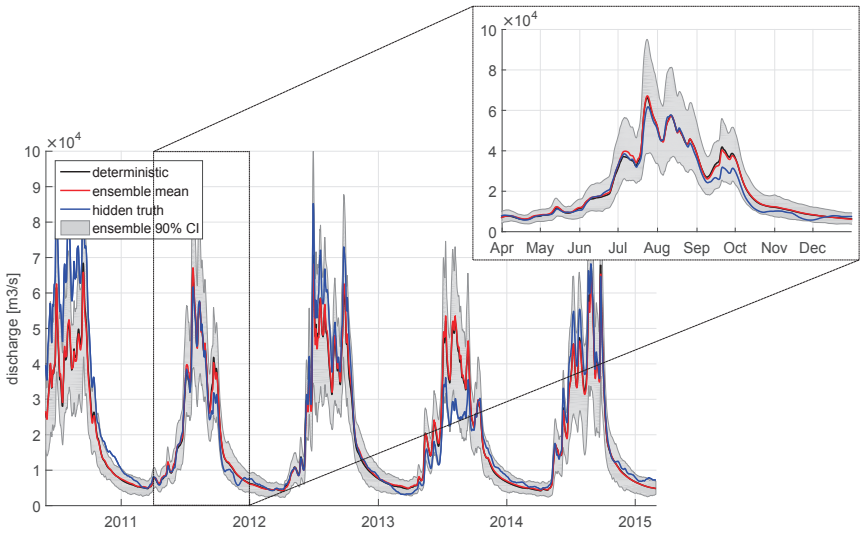

Figure 15. Result of the open loop run in terms of discharge at Bahadurabad station. Compared to HT 2.

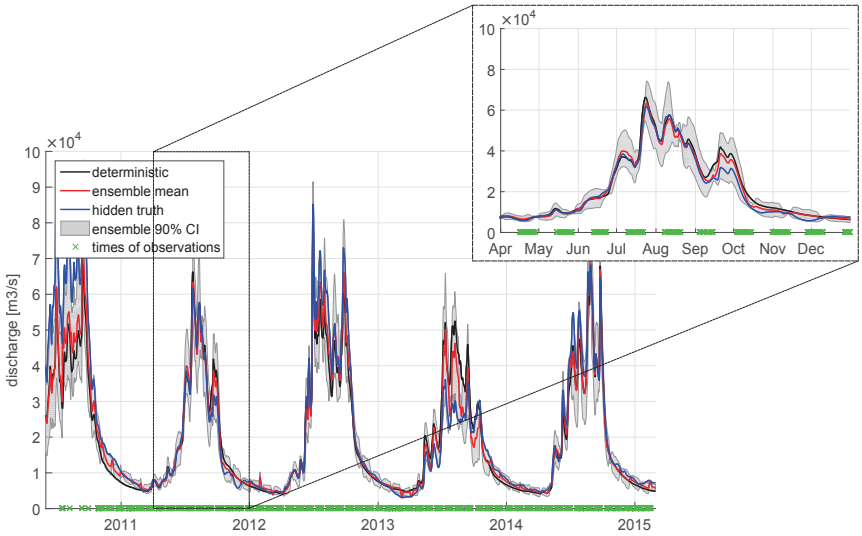

Figure 16. Result of the assimilation of synthetic CryoSat-2 observations from HT 2 with 0.2 m observation uncertainty, in terms of discharge at Bahadurabad station

Another aspect, that in this setup has a larger impact than the observation error, is the sampling pattern. This is illustrated in Figure 17: CryoSat-2, due to its orbit configuration with 30-day subcycles will cross the approximately

800 km long stretch of the Brahmaputra River on average daily during an approximately 12-day window. For the following approximately 18 days of its subcycle, no observations are available. Sentinel-3A, as an example of a short-repeat mission, exhibits a more regular sampling pattern with maximum gaps of 3.5 days between observations. These smaller gaps likely explain the superior performance of the Sentinel-3A data over the CryoSat-2 data, even though Sentinel-3A provides slightly fewer observations than CryoSat-2 (754 compared to 973 during the study period). Combining the sister missions Sentinel-3A and Sentinel-3B roughly doubles the number of available observations, further increasing data value. Also the direction of river flow in relation to ground track drift was investigated. The Brahmaputra River in the Assam valley flows from (north-) east to (south-) west (upwards along the y-axis in Figure 17), with flood wave travel speeds of 1 to 2.5 m s^{-1}. The ground track drift of CryoSat-2 has the same general direction, with a "travel speed" along the Brahmaputra River of roughly 0.7 m s^{-1}. Synthetic experiments allow setups where the flow direction of the river is changed to the opposite of the ground track drift. As can be seen in Table 7, this increases the data value of the assimilated CryoSat-2 observations. An explanation for this behaviour is that a flood wave traveling in the same direction as the ground track drift is more likely to be missed in the periods without observations than a flood wave travelling in the opposite direction of the ground track drift.

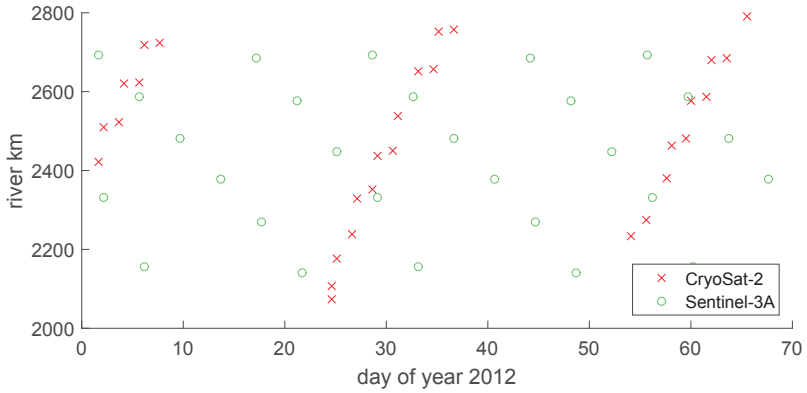

Figure 17. Sampling pattern of CryoSat-2 and Sentinel-3A along the Brahmaputra River in the Assam valley. For CryoSat-2 river transects with actually available observations are displayed; for Sentinel-3A all theoretical river transects are displayed. In reality, the number of observation from Sentinel-3A could be smaller.

8.5 Data Assimilation experiments with real data

DA experiments were also conducted with real CryoSat-2 observations. The model was evaluated against in situ discharge at Bahadurabad station, which was available during the high-flow seasons only. Table 8 summarizes some results.

Table 8. Results from DA experiments with real CryoSat-2 data, in terms of discharge at Bahadurabad station. Average of 4 runs in each row. The last column provides the CRPS improvement of the DA run compared to the open loop run.

	NSE [-]	sharp-ness [$m^3 s^{-1}$]	cover-age [-]	CRPS [$m^3 s^{-1}$]	CRPS change [%]
open loop	0.839	15264	0.926	3332	-
DA, cluster obs. unc. (mean 0.31 m)	0.839	11405	0.834	3244	3
DA, cluster obs. unc. scaled by 0.5	0.842	10741	0.784	3245	3
DA, obs. unc. 0.3 m*	0.871	9156	0.723	2997	10
DA, obs. unc. 0.15 m	0.874	8655	0.698	3021	9

* example run shown in **Figure 18**

The model uncertainty spread was well captured, as can be seen in the coverage of the open loop run which is close to the expected 90 %. DA runs were performed with the observation uncertainty derived from the actual spread of water level observations in the cluster groups. On average, their error was 0.31 m. This, however, did not lead to good assimilation results, which indicates that the spread of the individual observations is not a good indicator of observation uncertainty. Further DA runs with fixed observation uncertainty were performed, which showed improvements in terms of CRPS of up to 10 %. An example run with an observation uncertainty of 0.3 m is shown in Figure 18. Generally (also for the synthetic experiments), it can be seen that the assimilation decreases the coverage. The loss of coverage is, however, overcompensated by an increase in sharpness, leading to a better total model fit in terms of CRPS. Also the ensemble mean NSE is improving.

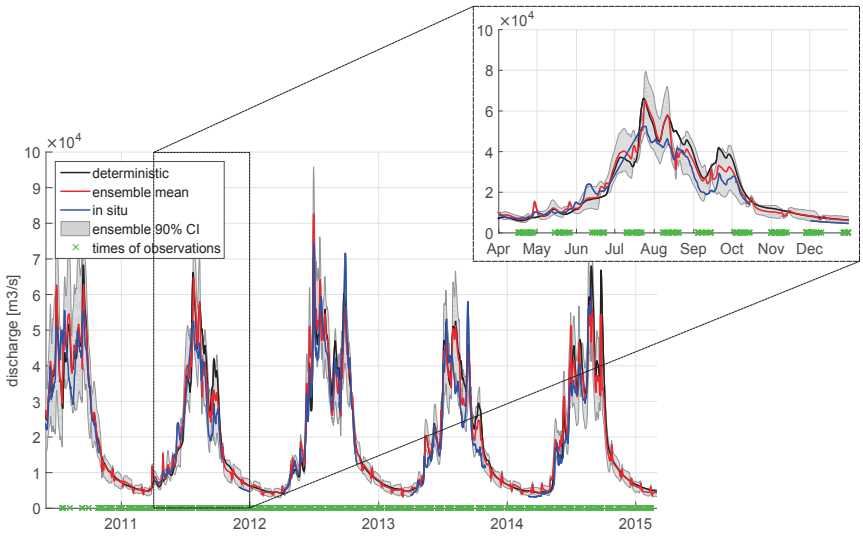

Figure 18. Results of a DA run with real CryoSat-2 data in terms of discharge at Bahadurabad station. Note that in situ data are only available during the high-flow seasons.

Improvements in terms of CRPS of up to 10 % obtained by assimilating real CryoSat-2 data have been considerably smaller than those obtained by assimilating synthetic CryoSat-2 data with up to 32 % in realistic scenarios. In principle, synthetic experiments are always expected to perform better, because all uncertainties are controlled. In the real case, these uncertainties have to be estimated. Observation uncertainty is unknown, as the CryoSat-2 data cannot be directly evaluated over the Brahmaputra River. The model uncertainty in the real case was assumed to originate from runoff forcing only. Even though the general model spread is realistic, the forcing error was modelled with Gaussian distributions, which may be unrealistic. A considerable amount of model uncertainty can be related to other parts of the model than its forcing, but for example uncertainties in the representation of the river bed, which for the Brahmaputra River is dynamic. This adds uncertainty to the simulated water level-discharge relationships. The water level-discharge relationships are a crucial part of this model setup, where observations of water level are assimilated, and results finally are evaluated in terms of discharge. Moreover, the in situ discharge values used as a benchmark are derived from rating curves, which inherently also bears uncertainty.

The improvements that could be obtained by assimilating real data are nonetheless in the range of what was obtained in similar previous studies. Michailovsky et al. (2013) improved the Interval Skill Score by around 5 % by assimilating Envisat altimetry data to a Muskingum routing scheme of the Brahmaputra River. Assimilating Envisat data to a model of the Amazon River, Paiva et al., (2013) improved the RMSE of discharge by up to 15 %.

9 Conclusions

The goal of this study was to evaluate CryoSat-2 satellite altimetry data over rivers, and evaluate their value in the parameterization and updating of hydrodynamic river models. CryoSat-2 has a unique orbit configuration, providing data with unprecedented spatial resolution along rivers. This could be shown to deliver added value even over dense in situ data. The work was based on two case studies, the well monitored Po River and the ungauged Brahmaputra River.

Level 2 CryoSat-2 altimetry data were filtered over river masks derived from Landsat imagery. Where necessary, the river masks were adapted yearly to reflect changes in the course of the river. Water level observations could be derived down to river widths around 100 m. Data availability was limited along the upstream Brahmaputra River, owing to rugged terrain in combination with the closed-loop control of the altimeter on CryoSat-2.

Water level observations from all three operation modes of CryoSat-2 were validated against in situ data over the Po River. The average RMSE between in situ and CryoSat-2 water level observations was found to be 0.38 m, well in the range of previous studies, especially over a narrow river like the Po. Performance did not differ substantially between the operation modes, which indicates good usability of CryoSat-2 data over many rivers globally.

For a hydrodynamic model of the Po River, CryoSat-2 was shown to be able to replace in situ data for channel roughness calibration. CryoSat-2 even allows for channel roughness calibration with higher spatial resolution than possible with the (already dense) network of in situ stations. Along the Brahmaputra River, CryoSat-2 data were used to calibrate the datums and shapes of synthetic cross sections. The calibrated model is assumed to accurately reproduce water level-discharge relationships. This is a prerequisite for the assimilation of distributed altimetry observations such as from CryoSat-2.

The DA framework integrated with the modelling software MIKE HYDRO River allows updating of river models with data with any kind of spatio-temporal distribution. This was demonstrated over the hydrodynamic model of the Brahmaputra River, assimilating CryoSat-2 data and other synthetic data. In synthetic experiments, the DA framework was used to investigate the effects of different observation sampling patterns and observation errors. It was shown that a regular temporal observation interval is beneficial. Synthetic data with the sampling pattern of CryoSat-2 improved discharge simula-

tions of the model in terms of CRPS by up to 32 %, while real data yielded improvements of up to 10 %. Part of the lower performance of the real data may be explained by issues with the cross section calibration.

This study can be seen as an effort to promote the to-date limited use of CryoSat-2 altimetry with its unique spatio-temporal sampling pattern in hydrology and to promote a move beyond the concept of virtual station altimetry in hydrology. Many of the current methods are in one way or the other limited to or at least optimized for data in the form of virtual station time series. New flexible methods of altimetry data processing, data distribution, and integration into river models that can be used with data with any kind of spatio-temporal distribution are needed.

10 Limitations and perspectives

There are a number of limitations to the presented methods, and ideas for future research and applications that arose during the work.

- Optical imagery for **river masking** is limited by cloud cover. In the Assam valley, it was only possible to derive one low-flow river mask per year, despite the 16-day return period of Landsat. Especially during the high-flow period, observations may have been missed. SAR imagery is an alternative which is not limited by cloud cover. Since the launch of the Sentinel-1A and -1B satellites in 2014 and 2016 it is freely available on global scale. Also, during the last years new global water mask services based on analysis of Landsat imagery became available, for example the Global Surface Water Explorer (Pekel et al., 2016), which promises to make full historic data of surface water extent available soon.
- Alternatively, discrimination between water and land returns could take place earlier in the data processing, i.e. during retracking (level 1b data). New research suggests that returns over rivers and land can be distinguished by **waveform classification** (Boergens et al., 2017b). This may address issues of the masking used in this work, for example the inherent inaccuracies of the ground location of altimetry data due to footprint size.
- The **calibrated synthetic, triangular cross sections** have, as mentioned, limited relation to the real river geometry. The method could be extended to other representations of cross section shape, for example freely varying between triangular and rectangular shape as suggested by Neal et al. (2015). Furthermore, river width information could be incorporated.
- The **developed DA framework** leaves room for further experiments. For example, assimilation of multi-mission datasets appears promising due to the large influence of sampling frequency on DA results. This could result in improved operational flood forecasting systems. Another aspect is the short memory of the states of the hydrodynamic model. Instead of updating only the hydrodynamic model, also the hydrologic model can be included in the update. The states of the rainfall-runoff models have a longer memory. For their updating other remote sensing data such as soil moisture could be used, which can address some of the uncertainty of precipitation forcing (Brocca et al., 2012, 2014).
- Synthetic DA experiments that can be conducted with the DA framework can **aid the design of future altimetry missions**. During this study, the

importance of sampling pattern and frequency was evaluated as well as the importance of observation error.

- A **more flexible view of satellite altimetry data in the hydrologic community**, i.e. not limited to virtual station data, does not only enable the addition of CryoSat-2 into existing databases and frameworks. It eases for example the use of data from short-repeat missions on specific beginning- or end-of-mission orbits (for example Envisat from 2010 to 2012), or the use of multi-mission altimetry. A change or an extension of common forms of distribution of altimetry data to the inland water community may be needed, for example to (filtered) level 2 data instead of aggregated level 3 data at virtual stations as it is more common today. In combination with innovative applications, such as CryoSat-2 data replacing in situ data in the calibration of the Po River model, use of satellite altimetry data can be extended, also in more engineering contexts.
- Development of more flexible data distribution and methods for combining altimetry data with river models has to be seen as a **preparation for the upcoming SWOT** mission. SWOT, planned to be launched in 2021, will provide fields of water heights along two 50 km-wide swaths instead of point observations.
- Finally, the combined efforts of hydrologists and remote sensing specialists in this field must lead to the development of an **operational, global hydrological model**, similar to what already exists for the oceans with MyOcean. This combines a model of river flow with remote sensing information. The model will be informed continuously by assimilating multi-mission altimetry observations and/or similar observations of, for example, water extent. Such a global hydrological model is of interest for climate change modelling, water resource management, etc.

11 References

Abbott, M. B. and Ionescu, F.: On The Numerical Computation Of Nearly Horizontal Flows, J. Hydraul. Res., 5(2), 97–117, doi:10.1080/00221686709500195, 1967.

Alsdorf, D. E., Rodríguez, E. and Lettenmaier, D. P.: Measuring Surface Water From Space, Rev. Geophys., 45, doi:10.1029/2006RG000197, 2007.

Andreadis, K. M., Clark, E. A., Lettenmaier, D. P. and Alsdorf, D. E.: Prospects for river discharge and depth estimation through assimilation of swath-altimetry into a raster-based hydrodynamics model, Geophys. Res. Lett., 34(10), L10403, doi:10.1029/2007GL029721, 2007.

Arnell, N. W. and Gosling, S. N.: The impacts of climate change on river flood risk at the global scale, Clim. Change, 134(3), 387–401, doi:10.1007/s10584-014-1084-5, 2016.

Barzaghi, R., Borghi, A., Carrion, D. and Sona, G.: Refining the estimate of the Italian quasi-geoid, Boll. di Geod. e Sci. Affin., 66(3), 2007.

Bates, P. D., Pappenberger, F. and Romanowicz, R. J.: Uncertainty in Flood Inundation Modelling, in Applied uncertainty analysis for flood risk management, edited by K. Beven and J. Hall, pp. 232–269, Imperial College Press, London (UK)., 2014.

Baup, F., Frappart, F. and Maubant, J.: Combining high-resolution satellite images and altimetry to estimate the volume of small lakes, Hydrol. Earth Syst. Sci., 18(5), 2007–2020, doi:10.5194/hess-18-2007-2014, 2014.

Becker, M., da Silva, J., Calmant, S., Robinet, V., Linguet, L. and Seyler, F.: Water Level Fluctuations in the Congo Basin Derived from ENVISAT Satellite Altimetry, Remote Sens., 6(10), 9340–9358, doi:10.3390/rs6109340, 2014.

Bercher, N., Calmant, S., Picot, N., Seyler, F. and Fleury, S.: Evaluation of Cryosat-2 Measurements for the Monitoring of Large River Water Levels, in Proceedings of 20 Years of Progress in Radar Altimetry, vol. SP-710, edited by L. Ouwehand, European Space Agency, Venice, Italy., 2013.

Berrisford, P., Dee, D., Fielding, K., Fuentes, M., Kallberg, P., Kobayashi, S. and Uppala, S.: The ERA-Interim Archive - Version 2.0., 2011.

Berry, P. A. M. and Benveniste, J.: Measurement of Inland Surface Water from Multi-mission Satellite Radar Altimetry: Sustained Global Monitoring for Climate Change, in Gravity, Geoid and Earth Observation, vol. 135, edited by S. P. Mertikas, pp. 221–229, Springer Berlin Heidelberg., 2010.

Berry, P. A. M., Garlick, J. D., Freeman, J. A. and Mathers, E. L.: Global inland water monitoring from multi-mission altimetry, Geophys. Res. Lett., 32(16), L16401, doi:10.1029/2005GL022814, 2005.

Biancamaria, S., Bates, P. D., Boone, A. and Mognard, N. M.: Large-scale coupled hydrologic and hydraulic modelling of the Ob river in Siberia, J. Hydrol., 379(1–2), 136–150, doi:10.1016/j.jhydrol.2009.09.054, 2009.

Biancamaria, S., Durand, M., Andreadis, K. M., Bates, P. D., Boone, A., Mognard, N. M., Rodríguez, E., Alsdorf, D. E., Lettenmaier, D. P. and Clark, E. A.: Assimilation of virtual wide swath altimetry to improve Arctic river modeling, Remote Sens. Environ., 115(2), 373–381, doi:10.1016/j.rse.2010.09.008, 2011a.

Biancamaria, S., Hossain, F. and Lettenmaier, D. P.: Forecasting transboundary river water elevations from space, Geophys. Res. Lett., 38, L11401, doi:10.1029/2011GL047290, 2011b.

Biancamaria, S., Lettenmaier, D. P. and Pavelsky, T. M.: The SWOT Mission and Its Capabilities for Land Hydrology, Surv. Geophys., 37(2), 307–337, doi:10.1007/s10712-015-9346-y, 2016.

Biancamaria, S., Frappart, F., Leleu, A.-S., Marieu, V., Blumstein, D., Desjonquères, J.-D., Boy, F., Sottolichio, A. and Valle-Levinson, A.: Satellite radar altimetry water elevations performance over a 200m wide river: Evaluation over the Garonne River, Adv. Sp. Res., 59, 128–146, doi:10.1016/j.asr.2016.10.008, 2017.

Birkinshaw, S. J., Moore, P., Kilsby, C. G., O'Donnell, G. M., Hardy, A. J. and Berry, P. A. M.: Daily discharge estimation at ungauged river sites using remote sensing, Hydrol. Process., 28(3), 1043–1054, doi:10.1002/hyp.9647, 2014.

Bishop, C. H., Etherton, B. J. and Majumdar, S. J.: Adaptive Sampling with the Ensemble Transform Kalman Filter. Part I: Theoretical Aspects, Mon. Weather Rev., 129(3), 420–436, doi:10.1175/1520-0493(2001)129<0420:ASWTET>2.0.CO;2, 2001.

Bjerklie, D. M., Dingman, S. L., Vorosmarty, C. J., Bolster, C. H. and Congalton, R. G.: Evaluating the potential for measuring river discharge from space, J. Hydrol., 278(1–4), 17–38, doi:10.1016/S0022-1694(03)00129-X, 2003.

Boergens, E., Buhl, S., Dettmering, D., Klüppelberg, C. and Seitz, F.: Combination of multi-mission altimetry data along the Mekong River with spatio-temporal kriging, J. Geod., 91(5), 519–534, doi:10.1007/s00190-016-0980-z, 2017a.

Boergens, E., Nielsen, K., Andersen, O. B., Dettmering, D. and Seitz, F.: Water levels of the Mekong River Basin based on CryoSat-2 SAR data classification, Hydrol. Earth Syst. Sci. Discuss., 1–22, doi:10.5194/hess-2017-217, 2017b.

Brakenridge, G. R., Cohen, S., Kettner, A. J., De Groeve, T., Nghiem, S. V., Syvitski, J. P. M. and Fekete, B. M.: Calibration of satellite measurements of river discharge using a global hydrology model, J. Hydrol., 475, 123–136, doi:10.1016/j.jhydrol.2012.09.035, 2012.

Brocca, L., Moramarco, T., Melone, F., Wagner, W., Hasenauer, S. and Hahn, S.: Assimilation of surface- and root-zone ASCAT soil moisture products into rainfall-runoff modeling, IEEE Trans. Geosci. Remote Sens., 50(7), 2542–2555, doi:10.1109/TGRS.2011.2177468, 2012.

Brocca, L., Ciabatta, L., Massari, C., Moramarco, T., Hahn, S., Hasenauer, S., Kidd, R., Dorigo, W., Wagner, W. and Levizzani, V.: Soil as a natural rain gauge: Estimating global rainfall from satellite soil moisture data, J. Geophys. Res. Atmos., 119, 5128–5141, doi:10.1002/2014JD021489, 2014.

Calmant, S. and Seyler, F.: Continental surface waters from satellite altimetry, Comptes Rendus Geosci., 338(14–15), 1113–1122, doi:10.1016/j.crte.2006.05.012, 2006.

Calmant, S., Seyler, F. and Cretaux, J. F.: Monitoring Continental Surface Waters by Satellite Altimetry, Surv. Geophys., 29(4–5), 247–269, doi:10.1007/s10712-008-9051-1, 2009.

Calmant, S., Crétaux, J.-F. and Rémy, F.: Principles of Radar Satellite Altimetry for Application on Inland Waters, in Microwave Remote Sensing of Land Surface, edited by

N. Baghdadi and M. Zribi, pp. 175–218, Elsevier., 2016.

Castellarin, A., Di Baldassarre, G. and Brath, A.: Floodplain management strategies for flood attenuation in the river Po, River Res. Appl., 27, 1037–1047, doi:10.1002/rra.1405, 2011.

Chelton, D. B., Ries, J. C., Haines, B. J., Fu, L.-L. and Callahan, P. S.: Satellite Altimetry, in Satellite Altimetry and Earth Sciences: A Handbook of Techniques and Applications, vol. 69, edited by L. Fu and A. Cazenave, pp. 1–131, Academic Press, San Diego., 2001.

Chow, V. T.: Open Channel Hydraulics, McGraw-Hill, New York., 1959.

Dee, D. P., Uppala, S. M., Simmons, A. J., Berrisford, P., Poli, P., Kobayashi, S., Andrae, U., Balmaseda, M. A., Balsamo, G., Bauer, P., Bechtold, P., Beljaars, A. C. M., van de Berg, L., Bidlot, J., Bormann, N., Delsol, C., Dragani, R., Fuentes, M., Geer, A. J., Haimberger, L., Healy, S. B., Hersbach, H., Hólm, E. V., Isaksen, L., Kållberg, P., Köhler, M., Matricardi, M., Mcnally, A. P., Monge-Sanz, B. M., Morcrette, J. J., Park, B. K., Peubey, C., de Rosnay, P., Tavolato, C., Thépaut, J. N. and Vitart, F.: The ERA-Interim reanalysis: Configuration and performance of the data assimilation system, Q. J. R. Meteorol. Soc., 137(656), 553–597, doi:10.1002/qj.828, 2011.

Dehecq, A., Gourmelen, N., Shepherd, A., Cullen, R. and Trouvé, E.: Evaluation of CryoSat-2 for height retrieval over the Himalayan range, in CryoSat-2 Third User Workshop, vol. SP-717, edited by L. Ouwehand, European Space Agency, Dresden, Germany., 2013.

DHI: MIKE 11 - A Modelling System for Rivers and Channels - Reference Manual, Hørsholm, Denmark., 2015.

Domeneghetti, A.: On the use of SRTM and altimetry data for flood modeling in data-sparse regions, Water Resour. Res., 52, 2901–2918, doi:10.1002/2014WR015716, 2016.

Domeneghetti, A., Tarpanelli, A., Brocca, L., Barbetta, S., Moramarco, T., Castellarin, A. and Brath, A.: The use of remote sensing-derived water surface data for hydraulic model calibration, Remote Sens. Environ., 149, 130–141, doi:10.1016/j.rse.2014.04.007, 2014.

Durand, M., Neal, J., Rodríguez, E., Andreadis, K. M., Smith, L. C. and Yoon, Y.: Estimating reach-averaged discharge for the River Severn from measurements of river water surface elevation and slope, J. Hydrol., 511, 92–104, doi:10.1016/j.jhydrol.2013.12.050, 2014.

European Space Agency and Mullard Space Science Laboratory: CryoSat Product Handbook., 2012.

Evensen, G.: Sequential data assimilation with a nonlinear quasi-geostrophic model using Monte Carlo methods to forecast error statistics, J. Geophys. Res., 99(C5), 10143, doi:10.1029/94JC00572, 1994.

Evensen, G.: The Ensemble Kalman Filter: theoretical formulation and practical implementation, Ocean Dyn., 53(4), 343–367, doi:10.1007/s10236-003-0036-9, 2003.

Evensen, G.: Data Assimilation - The Ensemble Kalman Filter, 2nd ed., Springer, Berlin Heidelberg., 2009.

Frappart, F., Calmant, S., Cauhopé, M., Seyler, F. and Cazenave, A.: Preliminary results of ENVISAT RA-2-derived water levels validation over the Amazon basin, Remote Sens. Environ., 100(2), 252–264, doi:10.1016/j.rse.2005.10.027, 2006.

Gao, H.: Satellite remote sensing of large lakes and reservoirs: from elevation and area to storage, Wiley Interdiscip. Rev. Water, 2, 147–157, doi:10.1002/wat2.1065, 2015.

Garambois, P.-A. and Monnier, J.: Inference of effective river properties from remotely sensed observations of water surface, Adv. Water Resour., 79, 103–120, doi:10.1016/j.advwatres.2015.02.007, 2015.

Garambois, P.-A., Calmant, S., Roux, H., Paris, A., Monnier, J., Finaud-Guyot, P., Montazem, A. and Santos da Silva, J.: Hydraulic visibility : using satellite altimetry to parameterize a hydraulic model of an ungauged reach of a braided river, Hydrol. Process., doi:10.1002/hyp.11033, 2016.

Getirana, A. C. V.: Integrating spatial altimetry data into the automatic calibration of hydrological models, J. Hydrol., 387(3–4), 244–255, doi:10.1016/j.jhydrol.2010.04.013, 2010.

Gleason, C. J. and Smith, L. C.: Toward global mapping of river discharge using satellite images and at-many-stations hydraulic geometry, Proc. Natl. Acad. Sci. U. S. A., 111(13), 4788–4791, doi:10.1073/pnas.1317606111, 2014.

Gneiting, T., Raftery, A. E., Westveld, A. H. and Goldman, T.: Calibrated Probabilistic Forecasting Using Ensemble Model Output Statistics and Minimum CRPS Estimation, Mon. Weather Rev., 133, 1098–1118, doi:10.1175/MWR2904.1, 2005.

Hall, A. C., Schumann, G. J.-P., Bamber, J. L., Bates, P. D. and Trigg, M. A.: Geodetic corrections to Amazon River water level gauges using ICESat altimetry, Water Resour. Res., 48, W06602, doi:10.1029/2011WR010895, 2012.

Havnø, K., Madsen, M. N. and Dørge, J.: MIKE 11 - A Generalized River Modelling Package, in Computer Models of Watershed Hydrology, edited by V. P. Singh, pp. 733–782, Water Resource Publications, Highlands Ranch, CO., 1995.

Hossain, F., Maswood, M., Siddique-E-Akbor, A. H., Yigzaw, W., Mazumdar, L. C., Ahmed, T., Hossain, M., Shah-Newaz, S. M., Limaye, A., Lee, H., Pradhan, S., Shrestha, B., Bajracahrya, B., Biancamaria, S., Shum, C. K. and Turk, F. J.: A promising radar altimetry satellite system for operational flood forecasting in flood-prone Bangladesh, IEEE Geosci. Remote Sens. Mag., 2(3), 27–36, doi:10.1109/MGRS.2014.2345414, 2014.

Hostache, R., Lai, X., Monnier, J. and Puech, C.: Assimilation of spatially distributed water levels into a shallow-water flood model. Part II: Use of a remote sensing image of Mosel River, J. Hydrol., 390(3–4), 257–268, doi:10.1016/j.jhydrol.2010.07.003, 2010.

Hunt, B. R., Kostelich, E. J. and Szunyogh, I.: Efficient data assimilation for spatiotemporal chaos: A local ensemble transform Kalman filter, Phys. D Nonlinear Phenom., 230(1–2), 112–126, doi:10.1016/j.physd.2006.11.008, 2007.

Jain, M., Andersen, O. B., Dall, J. and Stenseng, L.: Sea surface height determination in the Arctic using Cryosat-2 SAR data from primary peak empirical retrackers, Adv. Sp. Res., 55(1), 40–50, doi:10.1016/j.asr.2014.09.006, 2015.

Jain, S. K., Agarwal, P. K. and Singh, V. P.: Brahmaputra and Barak Basin, in Hydrology and Water Resources of India, vol. 57, pp. 419–472, Springer Netherlands, Dordrecht., 2007.

James, C. S.: Evaluation of Methods for Predicting Bend Loss in Meandering Channels, J. Hydraul. Eng., 120(2), 245–253, doi:10.1061/(ASCE)0733-9429(1994)120:2(245), 1994.

Jarihani, A. A., Callow, J. N., Johansen, K. and Gouweleeuw, B.: Evaluation of multiple

satellite altimetry data for studying inland water bodies and river floods, J. Hydrol., 505, 78–90, doi:10.1016/j.jhydrol.2013.09.010, 2013.

Jazwinski, A. H.: Stochastic Processes and Filtering Theory, Academic Press., 1970.

Jiang, L., Nielsen, K., Andersen, O. B. and Bauer-Gottwein, P.: Monitoring recent lake level variations on the Tibetan Plateau using CryoSat-2 SARIn mode data, J. Hydrol., 544(April 2010), 109–124, doi:10.1016/j.jhydrol.2016.11.024, 2017.

Kay, S. M.: Modern Spectral Estimation: Theory and Application, Prentice Hall., 1988.

Kleinherenbrink, M., Lindenbergh, R. C. and Ditmar, P. G.: Monitoring of lake level changes on the Tibetan Plateau and Tian Shan by retracking Cryosat SARIn waveforms, J. Hydrol., 521, 119–131, doi:10.1016/j.jhydrol.2014.11.063, 2015.

Lee, H., Yuan, T., Jung, H. C. and Beighley, E.: Mapping wetland water depths over the central Congo Basin using PALSAR ScanSAR, Envisat altimetry, and MODIS VCF data, Remote Sens. Environ., 159, 70–79, doi:10.1016/j.rse.2014.11.030, 2015.

Lettenmaier, D. P., Alsdorf, D., Dozier, J., Huffman, G. J., Pan, M. and Wood, E. F.: Inroads of remote sensing into hydrologic science during the WRR era, Water Resour. Res., 51(9), 7309–7342, doi:10.1002/2015WR017616, 2015.

Liu, Y., Weerts, A. H., Clark, M., Hendricks Franssen, H. J., Kumar, S., Moradkhani, H., Seo, D. J., Schwanenberg, D., Smith, P., Van Dijk, A. I. J. M., Van Velzen, N., He, M., Lee, H., Noh, S. J., Rakovec, O. and Restrepo, P.: Advancing data assimilation in operational hydrologic forecasting: Progresses, challenges, and emerging opportunities, Hydrol. Earth Syst. Sci., 16(10), 3863–3887, 2012.

Loucks, D. P. and van Beek, E.: Water Resources Systems Planning and Management. An Introduction to Methods, Models and Applications, United Nations Educational, Scientific and Cultural Organization, Paris., 2005.

Madsen, H. and Skotner, C.: Adaptive state updating in real-time river flow forecasting—a combined filtering and error forecasting procedure, J. Hydrol., 308(1–4), 302–312, doi:10.1016/j.jhydrol.2004.10.030, 2005.

Maillard, P., Bercher, N. and Calmant, S.: New processing approaches on the retrieval of water levels in Envisat and SARAL radar altimetry over rivers: A case study of the São Francisco River, Brazil, Remote Sens. Environ., 156, 226–241, doi:10.1016/j.rse.2014.09.027, 2015.

Markus, T., Neumann, T., Martino, A., Abdalati, W., Brunt, K., Csatho, B., Farrell, S., Fricker, H., Gardner, A., Harding, D., Jasinski, M., Kwok, R., Magruder, L., Lubin, D., Luthcke, S., Morison, J., Nelson, R., Neuenschwander, A., Palm, S., Popescu, S., Shum, C. K., Schutz, B. E., Smith, B., Yang, Y. and Zwally, J.: The Ice, Cloud, and land Elevation Satellite-2 (ICESat-2): Science requirements, concept, and implementation, Remote Sens. Environ., 190, 260–273, doi:10.1016/j.rse.2016.12.029, 2017.

Maybeck, P. S.: Introduction, Academic Press, New York, NY., 1979.

McCabe, M. F., Rodell, M., Alsdorf, D. E., Miralles, D. G., Uijlenhoet, R., Wagner, W., Lucieer, A., Houborg, R., Verhoest, N. E. C., Franz, T. E., Shi, J., Gao, H. and Wood, E. F.: The Future of Earth Observation in Hydrology, Hydrol. Earth Syst. Sci. Discuss., 1–55, doi:10.5194/hess-2017-54, 2017.

Md Ali, A., Solomatine, D. P. and Di Baldassarre, G.: Assessing the impact of different sources of topographic data on 1-D hydraulic modelling of floods, Hydrol. Earth Syst. Sci.,

19, 631–643, doi:10.5194/hess-19-631-2015, 2015.

Mersel, M. K., Smith, L. C., Andreadis, K. M. and Durand, M. T.: Estimation of river depth from remotely sensed hydraulic relationships, Water Resour. Res., 49(6), 3165–3179, doi:10.1002/wrcr.20176, 2013.

Michailovsky, C. I., McEnnis, S., Berry, P. A. M., Smith, R. and Bauer-Gottwein, P.: River monitoring from satellite radar altimetry in the Zambezi River Basin, Hydrol. Earth Syst. Sci., 16(7), 2181–2192, doi:10.5194/hess-16-2181-2012, 2012.

Michailovsky, C. I., Milzow, C. and Bauer-Gottwein, P.: Assimilation of radar altimetry to a routing model of the Brahmaputra River, Water Resour. Res., 49(8), 4807–4816, doi:10.1002/wrcr.20345, 2013.

Montanari, A.: Hydrology of the Po River: looking for changing patterns in river discharge, Hydrol. Earth Syst. Sci., 16(10), 3739–3747, doi:10.5194/hess-16-3739-2012, 2012.

Morvan, H., Knight, D., Wright, N., Tang, X. and Crossley, A.: The concept of roughness in fluvial hydraulics and its formulation in 1D , 2D and 3D numerical simulation models, J. Hydraul. Res., 46(2), 191–208, doi:10.1080/00221686.2008.9521855, 2008.

Neal, J., Schumann, G. and Bates, P.: A subgrid channel model for simulating river hydraulics and floodplain inundation over large and data sparse areas, Water Resour. Res., 48, W11506, doi:10.1029/2012WR012514, 2012.

Neal, J. C., Odoni, N. A., Trigg, M. A., Freer, J. E., Garcia-Pintado, J., Mason, D. C., Wood, M. and Bates, P. D.: Efficient incorporation of channel cross-section geometry uncertainty into regional and global scale flood inundation models, J. Hydrol., 529, 169–183, doi:10.1016/j.jhydrol.2015.07.026, 2015.

Nielsen, S. A. and Hansen, E.: Numerical simulation of the rainfall runoff process on a daily basis, Nord. Hydrol., 4, 171–190, 1973.

O'Loughlin, F., Trigg, M. A., Schumann, G. J. P. and Bates, P. D.: Hydraulic characterization of the middle reach of the Congo River, Water Resour. Res., 49(8), 5059–5070, doi:10.1002/wrcr.20398, 2013.

O'Loughlin, F. E., Neal, J., Yamazaki, D. and Bates, P. D.: ICESat-derived inland water surface spot heights, Water Resour. Res., 52(4), 3276–3284, doi:10.1002/2015WR018237, 2016.

Paiva, R. C. D., Collischonn, W., Bonnet, M.-P., de Gonçalves, L. G. G., Calmant, S., Getirana, A. and Santos da Silva, J.: Assimilating in situ and radar altimetry data into a large-scale hydrologic-hydrodynamic model for streamflow forecast in the Amazon, Hydrol. Earth Syst. Sci., 10(3), 2879–2925, doi:10.5194/hess-17-2929-2013, 2013.

Paiva, R. C. D., Durand, M. T. and Hossain, F.: Spatiotemporal interpolation of discharge across a river network by using synthetic SWOT satellite data, Water Resour. Res., 51, 430–449, doi:10.1002/2014WR015618, 2015.

Papa, F., Frappart, F., Malbeteau, Y., Shamsudduha, M., Vuruputur, V., Sekhar, M., Ramillien, G., Prigent, C., Aires, F., Pandey, R. K., Bala, S. and Calmant, S.: Satellite-derived surface and sub-surface water storage in the Ganges–Brahmaputra River Basin, J. Hydrol. Reg. Stud., 4, 15–35, doi:10.1016/j.ejrh.2015.03.004, 2015.

Pappenberger, F., Beven, K., Horritt, M. and Blazkova, S.: Uncertainty in the calibration of effective roughness parameters in HEC-RAS using inundation and downstream level

observations, J. Hydrol., 302(1–4), 46–69, doi:10.1016/j.jhydrol.2004.06.036, 2005.

Pekel, J.-F., Cottam, A., Gorelick, N. and Belward, A. S.: High-resolution mapping of global surface water and its long-term changes, Nature, 540(7633), 418–422, doi:10.1038/nature20584, 2016.

Pramanik, N., Panda, R. K. and Sen, D.: One dimensional hydrodynamic modeling of river flow using DEM extracted river cross-sections, Water Resour. Manag., 24(5), 835–852, doi:10.1007/s11269-009-9474-6, 2010.

Raney, K. R.: The delay/doppler radar altimeter, IEEE Trans. Geosci. Remote Sens., 36(5), 1578–1588, doi:10.1109/36.718861, 1998.

Reichle, R. H., Walker, J. P., Koster, R. D. and Houser, P. R.: Extended versus Ensemble Kalman Filtering for Land Data Assimilation, J. Hydrometeorol., 3(6), 728–740, doi:10.1175/1525-7541(2002)003<0728:EVEKFF>2.0.CO;2, 2002.

Ridler, M.-E., Madsen, H., Stisen, S., Bircher, S. and Fensholt, R.: Assimilation of SMOS-derived soil moisture in a fully integrated hydrological and soil-vegetation-atmosphere transfer model in Western Denmark, Water Resour. Res., 50(11), 8962–8981, doi:10.1002/2014WR015392, 2014.

Rosmorduc, V.: Hydroweb Product User Manual V1.0., 2016.

Rosmorduc, V., Benveniste, J., Bronner, E., Dinardo, S., Lauret, O., Maheu, C., Milagro, M. and Picot, N.: Radar Altimetry Tutorial, edited by J. Benveniste and N. Picot, 2011.

Sakov, P. and Bertino, L.: Relation between two common localisation methods for the EnKF, Comput. Geosci., 15(2), 225–237, doi:10.1007/s10596-010-9202-6, 2011.

Sakov, P. and Oke, P. R.: Implications of the Form of the Ensemble Transformation in the Ensemble Square Root Filters, Mon. Weather Rev., 136(3), 1042–1053, doi:10.1175/2007MWR2021.1, 2008.

Santos da Silva, J., Calmant, S., Seyler, F., Rotunno Filho, O. C., Cochonneau, G. and Mansur, W. J.: Water levels in the Amazon basin derived from the ERS 2 and ENVISAT radar altimetry missions, Remote Sens. Environ., 114(10), 2160–2181, doi:10.1016/j.rse.2010.04.020, 2010.

Schumann, G. J. P., Neal, J. C., Voisin, N., Andreadis, K. M., Pappenberger, F., Phanthuwongpakdee, N., Hall, A. C. and Bates, P. D.: A first large-scale flood inundation forecasting model, Water Resour. Res., 49(10), 6248–6257, doi:10.1002/wrcr.20521, 2013.

Schutz, B. E., Zwally, H. J., Shuman, C. A., Hancock, D. and DiMarzio, J. P.: Overview of the ICESat Mission, Geophys. Res. Lett., 32(21), L21S01, doi:10.1029/2005GL024009, 2005.

Schwatke, C., Dettmering, D., Bosch, W. and Seitz, F.: DAHITI – an innovative approach for estimating water level time series over inland waters using multi-mission satellite altimetry, Hydrol. Earth Syst. Sci., 19, 4345–4364, doi:10.5194/hess-19-4345-2015, 2015.

Sichangi, A. W., Wang, L., Yang, K., Chen, D., Wang, Z., Li, X., Zhou, J., Liu, W. and Kuria, D.: Estimating continental river basin discharges using multiple remote sensing data sets, Remote Sens. Environ., 179, 36–53, doi:10.1016/j.rse.2016.03.019, 2016.

Skøien, J. O. and Blöschl, G.: Spatiotemporal topological kriging of runoff time series, Water Resour. Res., 43(9), W09419, doi:10.1029/2006WR005760, 2007.

Song, C., Ye, Q., Sheng, Y. and Gong, T.: Combined ICESat and CryoSat-2 altimetry for accessing water level dynamics of Tibetan lakes over 2003-2014, Water, 7(9), 4685–4700, doi:10.3390/w7094685, 2015.

Sorooshian, S., Hsu, K., Coppola, E., Tomassetti, B., Verdecchia, M. and Visconti, G., Eds.: Hydrological Modelling and the Water Cycle: Coupling the Atmospheric and Hydrological Models, Springer., 2009.

Sun, W., Ishidaira, H. and Bastola, S.: Calibration of hydrological models in ungauged basins based on satellite radar altimetry observations of river water level, Hydrol. Process., 26(23), 3524–3537, doi:10.1002/hyp.8429, 2012.

Tarpanelli, A., Brocca, L., Barbetta, S., Faruolo, M., Lacava, T. and Moramarco, T.: Coupling MODIS and Radar Altimetry Data for Discharge Estimation in Poorly Gauged River Basins, IEEE J. Sel. Top. Appl. Earth Obs. Remote Sens., 8(1), 141–148, doi:10.1109/JSTARS.2014.2320582, 2015.

Tourian, M. J., Elmi, O., Chen, Q., Devaraju, B., Roohi, S. and Sneeuw, N.: A spaceborne multisensor approach to monitor the desiccation of Lake Urmia in Iran, Remote Sens. Environ., 156, 349–360, doi:10.1016/j.rse.2014.10.006, 2015.

Tourian, M. J., Tarpanelli, A., Elmi, O., Qin, T., Brocca, L., Moramarco, T. and Sneeuw, N.: Spatiotemporal densification of river water level time series by multimission satellite altimetry, Water Resour. Res., 52, 1140–1159, doi:10.1002/2015WR017654, 2016.

Tourian, M. J., Schwatke, C. and Sneeuw, N.: River discharge estimation at daily resolution from satellite altimetry over an entire river basin, J. Hydrol., 546, 230–247, doi:10.1016/j.jhydrol.2017.01.009, 2017.

Tropical Rainfall Measurement Mission Project (TRMM): Tropical Rainfall Measurement Mission Project (TRMM) 3-Hourly 0.25 deg. TRMM and Others Rainfall Estimate Data, 2011.

Villadsen, H., Andersen, O. B., Stenseng, L., Nielsen, K. and Knudsen, P.: CryoSat-2 altimetry for river level monitoring - Evaluation in the Ganges-Brahmaputra basin, Remote Sens. Environ., 168, 80–89, doi:10.1016/j.rse.2015.05.025, 2015.

Villadsen, H., Deng, X., Andersen, O. B., Stenseng, L., Nielsen, K. and Knudsen, P.: Improved inland water levels from SAR altimetry using novel empirical and physical retrackers, J. Hydrol., 537, 234–247, doi:10.1016/j.jhydrol.2016.03.051, 2016.

Vörösmarty, C. J., Green, P., Salisbury, J. and Lammers, R. B.: Global Water Resources: Vulnerability from Climate Change and Population Growth, Science (80-.)., 289(5477), 284–288, doi:10.1126/science.289.5477.284, 2000.

Wingham, D. J., Francis, C. R., Baker, S., Bouzinac, C., Brockley, D., Cullen, R., de Chateau-Thierry, P., Laxon, S. W., Mallow, U., Mavrocordatos, C., Phalippou, L., Ratier, G., Rey, L., Rostan, F., Viau, P. and Wallis, D. W.: CryoSat: A mission to determine the fluctuations in Earth's land and marine ice fields, Adv. Sp. Res., 37(4), 841–871, doi:10.1016/j.asr.2005.07.027, 2006.

World Water Assessment Programme: The United Nations World Water Development Report 3: Water in a Changing World, UNESCO and Earthscan, Paris, London., 2009.

Yan, K., Di Baldassarre, G. and Solomatine, D. P.: Exploring the potential of SRTM topographic data for flood inundation modelling under uncertainty, J. Hydroinformatics, 15(3), 849–861, doi:10.2166/hydro.2013.137, 2013.

Yan, K., Di Baldassarre, G., Solomatine, D. P. and Schumann, G. J.-P.: A review of low-cost space-borne data for flood modelling: topography, flood extent and water level, Hydrol. Process., 29, 3368–3387, doi:10.1002/hyp.10449, 2015.

Zannoni, E.: Ipotesi di potenziamento della capacità di laminazione del tratto medio-inferiore del Fiume Po attraverso una corretta gestione del sistema di arginature golenali, Università di Bologna., 2010.

12 Papers

I Jiang, L., Schneider, R., Andersen, O.B., Bauer-Gottwein, P., 2017. CryoSat-2 Altimetry Applications over Rivers and Lakes. Water 9, 211. doi:10.3390/w9030211

II Schneider, R., Tarpanelli, A., Nielsen, K., Madsen, H., Bauer-Gottwein, P. Evaluation of multi-mode CryoSat-2 altimetry data over the Po River against in situ data and a hydrodynamic model. *Manuscript submitted to Adv. Water Resour.*

III Schneider, R., Godiksen, P.N., Villadsen, H., Madsen, H., Bauer-Gottwein, P., 2017. Application of CryoSat-2 altimetry data for river analysis and modelling. Hydrol. Earth Syst. Sci. 21, 751–764. doi:10.5194/hess-21-751-2017

IV Schneider, R., Ridler, M.-E., Godiksen, P.N., Madsen, H., Bauer-Gottwein, P. A data assimilation system combining CryoSat-2 data and hydrodynamic river models. *Under revision. J. Hydrol.*

In this online version of the thesis, papers **I-IV** are not included but can be obtained from electronic article databases e.g. via www.orbit.dtu.dk or on request from

DTU Environment
Technical University of Denmark
Miljoevej, Building 113
2800 Kgs. Lyngby
Denmark

info@env.dtu.dk.

The Department of Environmental Engineering (DTU Environment) conducts science based engineering research within six sections: Water Resources Engineering, Water Technology, Urban Water Systems, Residual Resource Engineering, Environmental Chemistry and Atmospheric Environment.
The department dates back to 1865, when Ludvig August Colding, the founder of the department, gave the first lecture on sanitary engineering as response to the cholera epidemics in Copenhagen in the late 1800s.

Department of Environmental Engineering
Technical University of Denmark

DTU Environment
Bygningstorvet, building 115
2800 Kgs. Lyngby
Tlf. +45 4525 1600
Fax +45 4593 2850

www.env.dtu.dk